Evaporation of Ethanol/Iso-Octane Droplets (A Binary Component Fuel)

Minesh Vohra

A Thesis Submitted to

Indian Institute of Technology Hyderabad

In Partial Fulfillment of the Requirements for

The Degree of Master of Technology

भारतीय प्रौद्योगिकी संस्थान हैदराबाद
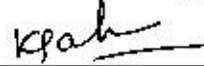
Indian Institute of Technology Hyderabad

Department of Mechanical Engineering

June 2011

Declaration

I declare that this written submission represents my ideas in my own words, and where ideas or words of others have been included, I have adequately cited and referenced the original sources. I also declare that I have adhered to all principles of academic honesty and integrity and have not misrepresented or fabricated or falsified any idea/data/fact/source in my submission. I understand that any violation of the above will be cause for disciplinary action by the Institute and can also evoke penal action from the sources that have thus not been properly cited, or from whom proper permission has not been taken when needed.

(Signature)

Minesh Vohra

Student Name

ME09G008

Roll No

Approval Sheet

This thesis titled "Evaporation Of Ethanol/Iso-Octane Droplets (A Binary Component Fuel)" by Mr. Minesh Vohra is approved for the degree of Master of Technology.

_____

Dr. Kirti Chandra Sahu

(Examiner)

Assistant Professor

Department of Chemical Engineering

IIT Hyderabad

_____

Dr. Abhay Sharma

(Examiner)

Assistant Professor

Department of Mechanical Engineering

IIT Hyderabad

_____

Dr. Raja Banerjee

(Advisor)

Assistant Professor

Department of Mechanical Engineering

IIT Hyderabad

_____

Dr. Saptarshi Majumdar

(Chairman)

Assistant Professor

Department of Chemical Engineering

IIT Hyderabad

Acknowledgements

I would like to express my profound respect for my supervisor Dr.Raja Banerjee. He is the person who has sculpted me to my current shape and has shown me the right direction to discover myself. The little work that I have done has been possible only because of his excellent guidance. Like a parent, he always kept a watchful eye on our needs and problems. During the two years of my M.Tech work, I never felt away from home owing to his parent-like company. I can say right from the deep of my heart that the guidance, I have received from him, is unprecedented. I am grateful to him for the valuable suggestions and inputs that he have provided from time to time.

Thanks to all C.A.E. Lab Staff, especially to Madhu Sir and Srikanth Sir and ma'am too, who helped me lot during my simulation work.

I am extremely lucky to have batchmates such as Prashant Uttambhai Patel, Rohan Barot IITM, Rahul Mishra IITB, Sudhir Arya IITM, Rajesh(Ph.D), Soma Shekara M A, Abhishek Anand, Chandrakant Kumar Nirala and to B.tech fellows too. I appreciate their patience to tolerate a disturbing person like me. The moral support that they have provided is unforgettable. Being with them is a nice experience that will be in the album of my memory for my entire life.

It is the time to take the name of my better half Ar.Manpreet Kaur. I am truly indebted to her for her inspiration, patience and sacrifices. Her company helped me to overcome many difficult situations. Her inspiration used to work like a tonic to revive my determination and self-confidence after any failure. Above all, she is a person who, I believe, has brought sood future for me. Finally, I thank everyone who helped me directly or indirectly during my stay at IIT Hyderabad.

Minesh Vohra

To

The God and My Loving Parents

Abstract

A numerical study has been performed to determine evaporation rate from the surface of a binary mixture of ethanol and iso-octane (i.e. E0, E10, E20, E85) flowing in 2D rectangular flow domain having dimensions $(400\text{x}533)\mu m^2$. The liquid and gas phases are flowing in counter-current direction. VOF multiphase model was used to model stratified two-phase flow. The vapour/liquid equilibrium pressure was calculated using SIMPLEC model. A parametric study with different inlet and exit conditions was performed.

Two dimensional flow domain subjected to boundary condition as velocity inlet and pressure outlet is modeled using ICEM CFD. This model is imported into commercial CFD solver ANSYS FLUENT 12.0.1, undergoing multiphase flow preceding with Vof model implemented upon a single Droplet and then on Multi-Droplet flow domain, keeping in mind that the droplet near to the inlet, evaporates earlier as compared to the droplet away from the inlet boundary.

The surrounding gas was either nitrogen or dry air. Numerical Simulations were conducted at standard atmospheric pressure and ambient temperatures from about 290 to 350 K. The initial droplet size was on the order of 20 μm. Mass transfer contributions from each component evaporating into the carrier gas was calculated and source terms were accordingly implemented in the continuity, momentum, energy and species equations. Source terms arising due to interfacial mass transfer are implemented in the continuity, momentum, energy and species equations.

Contents

List of Figures

List of Tables

Nomenclature

List of Symbols

ϕ_f	Face centered value.
ϕ	Cell centered value.
∇	Gradient.
Δs	Displacement vector.
ϕ	Face value.
A	Surface Area(m^2).
a_p	Linearized co-efficient.
a_{nb}	Linearized co-efficient of nb
$\alpha_1, \alpha_2, \alpha_q$	Volume Fraction of fluid.
C_p	Specific Heat(J/Kg K).
D, D_{ij}	Binary diffusivity(m/s^2).
E	Energy(J/Kg).
h	Enthalpy (J/Kg).
h_{fg}	Latent Heat of Vaporization (J/Kg).
h_w	Wall heat transfer coefficient.

J	Species flux (kg/m^{2}s).
K	Thermal Conductivity.
M	Molecular Weight(kg/m^{3}s).
P	Pressure(Pa).
$\dot{m}$	Mass transfer rate(Kg/s).
m_i'''	Mass transfer per unit Volume.
$S, S_e, S_m, S_{\alpha q}$	Source terms domain.
T	Temperature(k) domain.
t	Time(s).
u, v	Velocity (m/s).
V_{cell}	Volume of computational cell (m^3).
X	Liquid phase mole fraction.
x	Gas phase mole fraction.
y	Gas phase mass fraction.
Z	Compressibility factor.
$Subscripts$	:
i	Inlet.
e	Exit.
eff	effective.
g	Gas phase.
l	Liquid phase.

v	Vapor
C	Critical .

Superscripts :

i, j	i or jth species.
m	Mixture.

Chapter 1

Introduction

1.1 Background

For modern combustion engines using liquid fuels, several processes play important roles in reaching high efficiency in the combustion cycle and low emissions in the exhaust gas. Liquid fuel need to evaporated to form a proper vapour/air mixture for efficient combustion. For direct injection systems used in aircraft or car engines, the fuel enters the combustion chamber in the liquid state. The bulk liquid sheet of fuel needs to be breakdown into very small droplets because it helps in increase the surface to volume ratio. A high surface to volume ratio is required to increase the evaporation rate. Therefore fuel injectors are designed to atomize the fuel into fine droplets.

Hydrocarbon fuel is used to power anything, from cars to airplanes or even toy motor boats also. It is the lifeblood of our transportation system. As our technology advances, society is able to use several natural and man-made sources to power our vehicles. This summary will explore the different types of fuel and their properties.

1.1.1 Different Types of Fuel

Various types of fuels are used to drive the automobiles depending on the engine type. Fuels can be classified as :

- Regular Fuels

- Alternative Fuels

Regular Fuels:

- **Petrol(Gasoline)** :

Gasoline, or petrol, is a translucent, yellow-tinted liquid mixture, derived from petroleum, which is primarily used as a fuel in internal combustion engines. It consists mostly of aliphatic hydrocarbons obtained by the fractional distillation of petroleum, enhanced with iso-octane or the aromatic hydrocarbons like toluene and benzene to increase its octane rating. Small quantities of various additives are common, for the purpose of tuning engine performance or reducing harmful exhaust emissions. Some mixtures also contain significant quantities of ethanol as a partial alternative fuel. Gasoline is more volatile than diesel oil, Jet-A or kerosene, not only because of the base constituents, but also because of the additives added to it. The desired volatility depends on the ambient temperature. In hot weather, gasoline components of higher molecular weight and thus lower volatility are used. In cold weather, too little volatility results in cars failing to start.The specific gravity (or relative density) of gasoline ranges from 0.71-0.77 (719.7 kg/m3), higher densities having a greater volume of aromatics.

PULP is a special blend of petrol designed to bring high octane, and hence high engine power, as well as knock- free performance to unleaded cars with a high-octane requirement. PULP has a Research Octane Number (RON)of 95. RON is determined by running the fuel in a test engine with a variable, compression ratio under controlled conditions, and comparing the results with those for mixtures of iso-octane and n-heptane.

98 RON has a Research Octane Number (RON) of 98. It is a high-octane unleaded fuel that maximizes engine power and performance, as well as producing less pollution. It has low levels of benzene, sulphur and lower aromatic and a sulphur content which is 10 times lower than the national standard for unleaded fuels.

- <u>Diesel</u>:

  Diesel fuel in general is any liquid fuel used in diesel engines. The most common is a specific fractional distillate of petroleum fuel oil, but alternatives that are not derived from petroleum, such as biodiesel, biomass to liquid (BTL) or gas to liquid (GTL) diesel, are increasingly being developed and adopted. To distinguish these types, petroleum-derived diesel is increasingly called Petrodiesel. Petrodiesel's higher density results in higher greenhouse gas emissions per litre compared to gasoline, the 20-40 % better fuel economy achieved by modern diesel-engined automobiles offsets the higher per-litre emissions of greenhouse gases, and a diesel-powered vehicle emits 10-20 percent less greenhouse gas than comparable gasoline vehicles.A disadvantage of diesel as a vehicle fuel in some climates, compared to gasoline or other petroleum-derived fuels, is that its viscosity increases quickly as the fuel's temperature decreases, turning into a nonflowing gel at temperatures as high as -19°C (-2.2°F) or -15°C (5°F), which cannot be pumped by regular fuel pumps. Special low-temperature diesel contains additives to keep it in a more liquid state at lower temperatures, yet starting a diesel engine in very cold weather may still pose considerable difficulties. Petroleum-derived diesel is composed of about 75% saturated hydrocarbons (primarily paraffins including n, iso, and cycloparaffins), and 25% aromatic hydrocarbons (including naphthalenes and alkylbenzenes). The average chemical formula for common diesel fuel is $C_{12}H_{23}$, ranging approximately from $C_{10}H_{20}$ to $C_{15}H_{28}$.

  Diesel engines, DEISEL as a fuel are usually very efficient engines, offering better fuel economy in comparison to equivalent petrol models. Diesel engines emit very low levels of exhaust hydrocarbons and carbon monoxide when correctly tuned and maintained. The main concern diesel engines raise particulate emmision, which can be a health hazard.

Alternative Fuels:

Alternative fuel technology with respect to regular fuels will become more common in coming decades. Rising fuel prices and regulations aimed at reducing carbon dioxide

emissions on the part of some regulatory agencies made it desirable to improve the efficiency of internal combustion engines used in both the automotive and heavy equipment industries. Diesel engines have long been favored for heavy equipment and over the road trucking applications owing to their higher efficiency and durability compared with spark ignition (SI) engines. Future standards however require substantial reductions in NOx and particulate emissions, necessitating costly particulate filters and lean NOx catalysts. There is an urge for the alternative fuels to alleviate the energy crisis. For the past few decades, efforts have been made to commercialize various alternative fuels such as biodiesel, alcohol, DME, CNG, LPG and hydrogen.

Alternative fuels are classified as:

- Bio-Deisel:

  Biodiesel is a fuel that is made from waste vegetable oil(cooking oil). It can be used in place of petroleum diesel fuel for vehicles or heating oil for buildings.Biodiesel fuel is made from oils or fats, which are both hydrocarbons, most commonly soybean oil. These hydrocarbons are filtered, then mixed with an alcohol, which is usually methanol, and a catalyst (sodium or potassium hydroxide). The major products of this reaction are the biodiesel fuel, which is an ester, and glycerol, which has commercial uses, such as in cosmetics.

  Biodiesel is designated by the letter B and a number representing the percent of the fuel that is biodiesel. The rest of the fuel is petroleum diesel. For example, a mixture of 20% biodiesel and 80% petroleum diesel would be labeled B20. This ratio of biodiesel to petroleum diesel is commonly used. Biodiesel is 100% biodiesel fuel and is referred to as B100 or "neat biodiesel". Biodiesel is made from natural renewable sources and can be blended in almost any ratio with petroleum based diesel. Biodiesel has viscosity close to diesel. Biodiesel blends are often known by the ratio of biodiesel to regular diesel i.e. B20 means 20% biodiesel and 80% petroleum based diesel. The most common blends available internationally are B5 (a mix of 5% biodiesel and 95% petroleum based diesel) and B20 (a mix of 20% biodiesel and 80% petroleum based diesel). Since the majority of modern diesel en-

gines have direct injection (DI) fuel systems, these engines are more sensitive to fuel spray characteristics compared to indirect injection engines. According to Government of India(GOI) National Policy of Bio-Fuels, bio-fuels derived from indigenous non-food feed-stock have been recognized as an important alternative fuel that can supplement petroleum based fuels for the transportation sector. According to GOI policy statement, bio-fuels will be derived solely from non-food feed-stock raised on degraded or wastelands that are not suited for agriculture. Bio-fuels derived from such sources have the following advantages:

- Renewable type of fuel

- Environmentally friendly

- Provides strategic energy security to the country

- Stimulate rural growth

- Avoiding possible conflict of fuel v/s food competition

- Ethanol:

  Ethanol is a naturally occurring gas that is usually found in small parts with other natural gases. However, ethanol can also be manually produced and used as fuel. Ethanol production includes the fermentation of corn stalks or sugar cane. Although ethanol burns cleaner than traditional gasoline, costs are equivalent to gasoline and fuel efficiency is more than a third less efficient.

- Natural Gas:

  Natural gas refers to methane-based gas found in coal beds. It can also be found in landfills, bogs and marshes because of special organisms called methanogens. Before being used as a fuel, natural gas must go through extensive processing to remove all of the other associated chemicals until only the methane is left.

- Hydrogen Fuel:

There are chemical reactions that can also produce energy that can be used as fuel. Hydrogen fuel is one example. Oxygen and hydrogen are combined in a proton exchange fuel cell. When the two are chemically combined, they can produce electricity that is used as fuel, creating water and vapors as a byproduct.

- Straight Vegetable Oil:

  A fast food restaurant leftover, straight vegetable oil (SVO) can also act as a fuel. Typical fuel prosperities of vegetable oils indicates that the kinetic viscosity of most of the SVO.s varies in the range of 30-40 cSt at 40°C. High viscosity of vegetable oils (30-200cSt @40°C) as compared to mineral diesel (4 cSt @ 40°C) leads to unsuitable pumping and fuel spray characteristics [5]. Larger size fuel droplets are injected from injector nozzle instead of a spray of fine droplets, which leads to inadequate air-fuel mixing. Poor atomization, lower volatility, and inefficient. The high viscosity of these oils is due to their large molecular mass (in the range of 600-900), which is approximately four times higher than the conventional diesel fuel. Vegetable oils have comparable energy content, cetane number, heat of vaporization and stoichiometric air-fuel ratio as that of mineral diesel.

- Liquefied Petroleum Gas(LPG):

  LPG, most commonly a blend of propane and butane, is an environmentally cleaner fuel compared to petrol and diesel. It is the most widely accepted alternative fuel for the automotive sector.
  Despite LPG cars having lower fuel economy compared to petrol-powered vehicles, fuel costs will usually be lower, as retail LPG prices tend to be lower than other fuel products.

- Lead Replacement Petrol(LRP):

  LRP (96 RON) was introduced as an environmental alternative for cars that used leaded petrol. LRP was refined to contain no lead, along with lower concentrations of benzene and sulphur, respectively identified as health hazards and pollutants. Lead was historically added to petrol as a cost-effective way of increasing octane

and hence engine power rating and providing a measure of engine protection by way of its lubricating qualities.

Petroleum is still the number one fuel source used to power industrial nations. Petroleum is also known as crude oil. It is found in large reservoirs throughout the Earth. Petrol is usually taken to a refinery that turns it into usable forms, such as Gasoline.

1.1.2 Fuel Injection Systems

Fuel injection is a system for mixing fuel with air in an internal combustion engine.It has become the primary fuel delivery system used in automotive petrol engines. A fuel injection system is designed and calibrated specifically for the type(s) of fuel it will handle. Most fuel injection systems are for gasoline or diesel applications.

In case of automotive engines a continuous metered quantity of the gasoline-air mixture must be ensured to make the engine run smoothly. In a gasoline injection system, the fuel is injected into intake manifold or near the intake port through an injector. Gasoline is received by the injector from the pump and is sprayed into the air stream in a finely atomized form. Compared to carburetion the mixing of gasoline with the air stream is better in this case due to better control of the system.

Types of Injection Systems

With the advent of electronic fuel injection (EFI), the diesel and gasoline hardware has become similar. EFI's programmable firmware has permitted common hardware to be used with different fuels.Carburetors were the predominant method used to meter fuel on gasoline engines before the widespread use of fuel injection. A variety of injection systems have existed since the earliest usage of the internal combustion engine.

The primary difference between carburetors and fuel injection is that fuel injection atomizes the fuel by forcibly pumping it through a small nozzle under high pressure, while a carburetor relies on low pressure created by intake air rushing through it to add the fuel to the airstream.The fuel injector is only a nozzle and a valve: the power to inject the

fuel comes from a pump or a pressure container farther back in the fuel supply. The fuel injection systems are classified as:

- **Single-point injection/ Throttle-body injection(TBI)**:

  This is the earliest and simplest type of fuel injector. Single-point injectors simply replaces the carburetor with one or two fuel-injector nozzles in the throttle body, which is the throat of the engines air intake manifold. For some automakers, single-point injection was a stepping stone to the more complex multi-point system. Though not as precise as the systems that have followed, TBI meters fuel better than a carburetor and is less expensive and easier to service.

  The SPI system injects fuel at the throttle body (the same location where a carburetor introduced fuel). The induction mixture passes through the intake runners like a carburetor system, and is thus labeled a "wet manifold system". Fuel pressure is usually specified to be in the range of 0.69-1.03 bar. The justification for single-point injection was low cost. Many of the carburetor's supporting components could be reused such as the air cleaner, intake manifold, and fuel line routing. This postponed the redesign and tooling costs of these components. Most of these components were later redesigned for the next phase of fuel injection's evolution, which is individual port injection, commonly known as MPFI or "multi-point fuel injection".

- **Central port injection (CPI)**:

  This system is also known as 'Central Port Fuel Injection'. It uses tubes with poppet valves from a central injector to spray fuel at each intake port rather than the central throttle-body. The two variants were CPFI from 1992 to 1995, and CPSI from 1996 onwards. CPFI is a batch-fire system, in which fuel is injected to all ports simultaneously. The later CSI system, sprayed fuel sequentially.

- **Multi-point fuel injection**:

  Multi-point fuel injection injects fuel into the intake ports just upstream of each cylinder's intake valve, rather than at a central point within an intake manifold.

MPFI (or just MPI) systems can be sequential, in which injection is timed to coincide with each cylinder's intake stroke; batched, in which fuel is injected to the cylinders in groups, without precise synchronization to any particular cylinder's intake stroke; or simultaneous, in which fuel is injected at the same time to all the cylinders. The intake is only slightly wet, and typical fuel pressure runs between 2.76-3.45 bar.

Multi-point fuel injection devotes a separate injector nozzle to each cylinder, right outside its intake port, which is why the system is sometimes called port injection. Shooting the fuel vapor close to the intake port almost ensures that it will be drawn completely into the cylinder.

The main advantage is that MPFI meters fuel more precisely than TBI designs, better achieving the desired air/fuel ratio and improving all related aspects. Also, it virtually eliminates the possibility that fuel will condense or collect in the intake manifold.

- **Sequential fuel injection (SFI)**:

  Sequential fuel injection, also called sequential port fuel injection (SPFI) or timed injection, is a type of multi-port injection. Though basic MPFI employs multiple injectors, they all spray their fuel at the same time or in groups. As a result, the fuel may hang around a port for as long as 150 milliseconds when the engine is idling. This may not seem like much, but it is enough of a shortcoming that engineers addressed it: Sequential fuel injection triggers each injector nozzle independently. Timed like spark plugs, they spray the fuel immediately before or as their intake valve opens. It seems a minor step, but efficiency and emissions improvements come in very small doses.

- **Direct Injection**:

  Direct fuel injection costs more than indirect injection systems: the injectors are exposed to more heat and pressure, so more costly materials and higher-precision electronic management systems are required. However, the entire intake is dry, making this a very clean system. In a common rail Deisel Injection (CRDi) system, the fuel from the fuel tank is supplied to the common header (called the accumula-
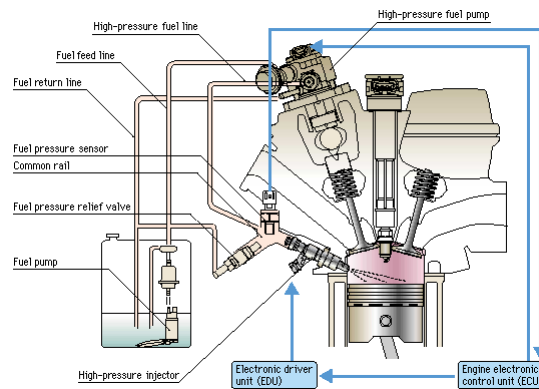
Figure 1.1: Gasoline Direct Injection System

tor). This fuel is then sent through tubing to the injectors which inject it into the combustion chamber. The header has a high pressure relief valve to maintain the pressure in the header and return the excess fuel to the fuel tank.The fuel is sprayed with the help of a nozzle which is opened and closed with a needle valve, operated with a solenoid. When the solenoid is not activated, the spring forces the needle valve into the nozzle passage and prevents the injection of fuel into the cylinder. The solenoid lifts the needle valve from the valve seat, and fuel under pressure is sent in the engine cylinder. Third-generation common rail diesels use piezoelectric injectors for increased precision, with fuel pressures up to 1,800 bar.

Need of GI engines instead of carburetion in automotive engines because of following reasons:

1. To have uniform distribution of fuel in a multi cylinder engine.

2. To improve breathing capacity i.e.Volumetric efficiency.

3. To reduce or eliminate detonation.

4. To prevent fuel loss during scavenging in case of two-stroke engines.

Referring to the Fig.[1.2(a)] Here it shows Intake-air pathlines through the intake valves, In Fig.[1.2(b)] Shows Fuel injection and vaporization from a multihole fuel injector. Liquid fuel is colored by drop temperature, and fuel vapor is indicated
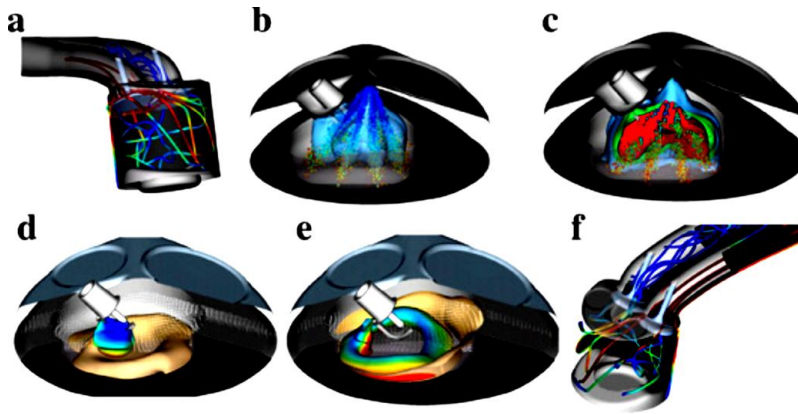
Figure 1.2: Physical Process In DI Engine[1]

by transparent blue, In Fig.[1.2(c)] Mixture preparation through interactions between fuel spray and in-cylinder gas motion, In Fig.[1.2(d)] Spark ignition and early flame kernel growth, In Fig.[1.2(e)] Partially premixed flame propagation and In Fig.[1.2(f)] Exhaust flow containing pollutants (UHC, NO_x, soot) to downstream catalytic after treatment system.

Presently GDI systems are used in both two-strokes as well as four-stroke engines now these days. In two storkes engines GDI is used that is low-pressure air-assisted, and high-pressure. The benefits of direct injection are even more pronounced in two-stroke engines, because it eliminates much of the pollution they cause. With direct injection, only air comes from the crankcase, and fuel is not injected until the piston rises and all ports are closed.In conventional two-strokes, the exhaust and intake ports are both open at the same time, at the bottom of the piston stroke.A large portion of the fuel/air mixture entering the cylinder from the crankcase through the intake ports goes directly out, unburned, through the exhaust port. Here showing below various types of injection system depending upon the location of fuel injector
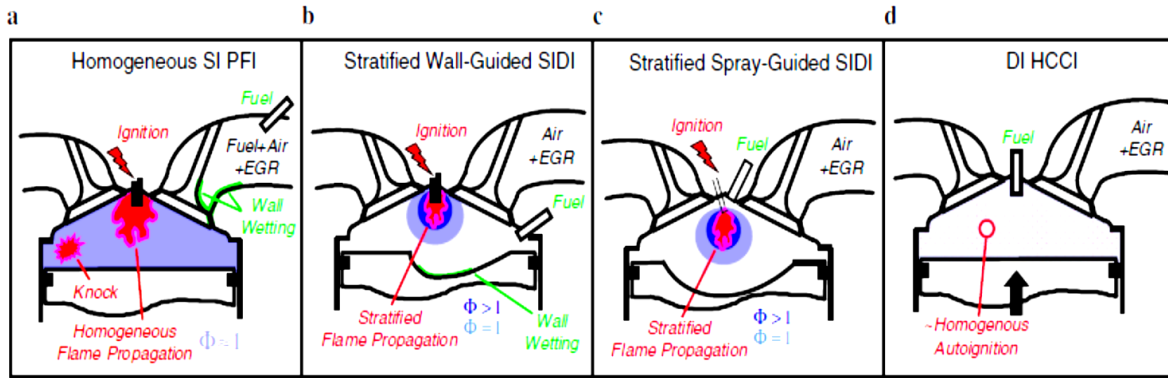
Figure 1.3: Gasoline engine types classified by fuel injector location, mixture formation process, ignition model, and combustion mode (a) Port-Fuel Injection(PFI), (b) Wall-Guided Spark Ignition Direct Injection (WG-SIDI), (c) Spray Guided Spark Ignition Direct Injection (SG-SIDI), (d) Homogeneous Charge Compression Ignition(HCCI)[1].

1.1.3 Air Fuel Ratio - Atomization

Air-fuel ratio (AFR) is the mass ratio of air to fuel present in an internal combustion engine. If enough air is provided to completely burn all of the fuel, the ratio is known as the stoichiometric mixture. AFR is an important measure for anti-pollution and performance tuning reasons. A stoichiometric mixture unfortunately burns very hot and can damage engine components if the engine is placed under high load at this fuel air mixture. Due to the high temperatures at this mixture, detonation of the fuel air mix shortly after maximum cylinder pressure is possible under high load (referred to as knocking or pinging). Detonation can cause serious engine damage as the uncontrolled burning of the fuel air mix can create very high pressures in the cylinder. As a consequence stoichiometric mixtures are only used under light load conditions. For acceleration and high load conditions, a richer mixture (lower air-fuel ratio) is used to produce cooler combustion products and thereby prevent detonation and overheating of the cylinder head.

Atomization refers to breakup of liquid fuel into fine droplets. The droplet sizeis several orders smaller than nozzle diameter. Atomization phenomenon also termed as the first phase in obtaining proper mixing of fuel and air in combustion chamber. The fuel must be properly distributed, or dispersed,in desired region of the combustion chamber. Some of the important factors which controls atomization process are:

12

1. **Injection Pressure**

2. **Density of air in Cylinder**

3. **Physical properties of fuel**

4. **Nozzle Design**

5. **Temperature inside Cylinder**

High injection pressure results in finer liquid droplet and greater penetration depth of the fuel into combustion chamber. The droplet size distribution strongly depends on the aerodynamic instability during the primary and secondary jet breakup. Aerodynamic instability, which in turn depends on velocity of the liquid sheet and fuel droplet, is a direct function of the injection pressure. It also produces fine droplets which tends to mix more readily with air. The greater the density of compressed air in the combustion chamber,the greater the resistance offered to fuel droplets in the chamber, which results in better atomization. The physical qualities of fuel itself, such as viscosity, surface tension, etc., also affect dispersion of fuel. The nozzle must spray the fuel into the chamber in such a manner as to minimize the quantity of fuel reaching the surrounding walls. Any fuel striking the wall results in producing in film of liqiud fuel. This causes increased unburnt hydrocarbons emission which in turn reduce engine efficiency. The design of nozzle is closely interrelated to the type of combustion chamber used. Turbulent type of combustion chamber depends upon the required mixing of fuel and air. The non-turbulent type of chamber on the other hand depends almost entirely on both the nozzle design and injection pressure to secure the desired mixing in the combustion chamber i.e.air-fuel ratio.

Spray Formation and Droplet Size Distribution

In order to improve fuelair mixing, it is important to understand the fuel atomization and spray formation processes. The various phase of spray formation as the fuel is injected through the nozzle is shown below. At the start the pressure difference across the orifice is low. Therefore single droplets are formed as in Fig.[1.4(a)]. As pressure difference
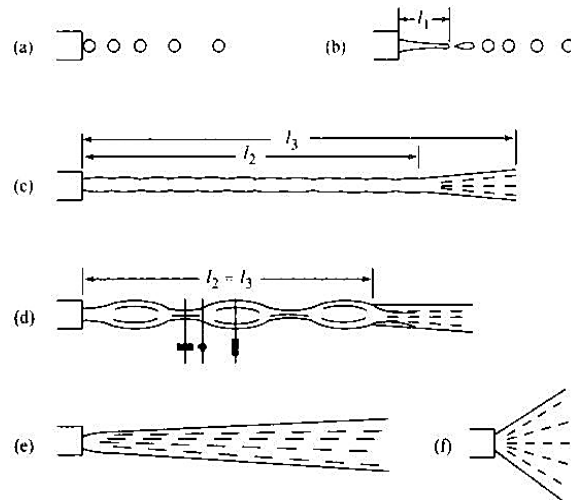
Figure 1.4: Spray Formation[2]

increases the following process occurs sequentially.

- A stream of fuel emerges from nozzle having some breakage length (l_1) as shown in Fig.[1.4(b)].

- The stream encounter Aerodynamic resistance from the dense air present in the chamber(12 to 14) times the ambient pressure) and breaks into a spray,say at a distance $l_3$as shown in Fig.[1.4(c)].

- With further increase in pressure difference the breakup distance decreases and cone angle increases until the apex of the cone practically coincides with orifice Fig [1.4(d),(e) and (f)].

Larger droplets provide a higher penetration into a chamber but smaller droplets at the outskirts of spray are required for quick mixing and evaporation of fuel. The diameter of most of the droplet in spray is less than 5 microns for particular class of nozzles. The droplet size depends on various factors as listed below :-

1. Mean droplet size increase with decrease in injection pressure.

2. Mean droplet size decrease with increase in air density.

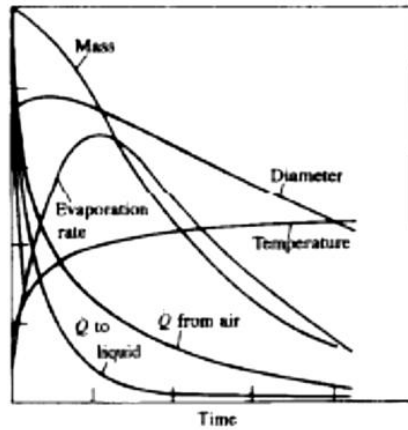3. Mean droplet size increase with increase in fuel viscosity.

14

Figure 1.5: Evaporation process at the time of injection[2]

4. Size of droplet increases with increase in dia. of nozzle.

.

1.1.4 Droplet Evaporation Phenomenon

The droplet evaporation phenomenon undergo three phases at ambient temperature stated below :

- Deceleration of drop due to Aerodynamic Drag.

- Heat Transfer to drop from ambeint air.

- Mass transfer of vaporized fuel away from drop.

As the droplet temperature increase due to heat transfer, the fuel vapor pressure increases and evaporation rate increases. As mass transfer rate of vapor away from the drop increases, the fraction of heat transferred to the drop surface which in available to increase further the drop temperature decreases. As the drop velocity decreases, the convective heat transfer co-efficient between the air and drop decreases. The combination of these factors gives the behavior as shown in Fig.[1.5].

Commercial fuels are complex mixtures of many compounds with different physical properties. For that reason, the evaporation of multi-component droplets is a complex process. As the droplets travel through the combustion chamber, their size and composition

15

changes. The size history influences the dynamic behavior of the droplets, whereas the variation of the composition determines the distribution of the gasified fuel compounds within the combustion chamber. The fundamental understanding of these processes is essential for the modeling of fuel sprays. In fuel sprays, droplet evaporation is influenced by several effects such as convection of the surrounding gas flow or an interaction among droplets.

Evaporation of fuel droplets is a complex process which depends on several factors; some of the important factors being composition of fuel, injection pressure, ambient pressure and temperature, sensible and latent heat transfer, etc. During normal operation of an engine, the inlet port and cylinder temperature is at an elevated temperature as compared to the injected fuel temperature. Therefore, there is sensible heat transfer from the surrounding air to the fuel. However, evaporation of fuel droplet results in evaporative cooling due to latent heat transfer. Hence, the rate of change of fuel temperature is strongly dependent on these contradicting heat transfer process and on the fuel composition. Alcohol/gasoline is a high non-ideal with the mixture vapour pressure much higher than the vapour pressure of the individual components. Therefore, latent heat transfer of alcohol/iso-octane is higher than pure gasoline. Additionally, surface tension of fuel droplet is dependent on droplet temperature. As can be seen from the above arguments, droplet evolution directly depends on surface tension, sensible and latent heat transfer.

Chapter 2

Literature Survey

2.1 Literature Survey

As an alternative fuel, Alcohol blended gasoline is increasingly used for automative SI Engines because ethanol can be obtained from renewable resources like sugarcane etc.. For engine to be work efficiently, fuel plays an important role depending upon the various properties of fuel as well as engine's internal conditions i.e. operating temperature, pressure. Alcohols like ethanol have lower molecular weight that the mean molecular weight of gasoline which adversely effects the volumetric efficiency of the engine. However, latent heat of ethanol is higher than that of gasoline which results in higher evaporative cooling and therefore compensates the loss the volumetric efficiency with increased charge density inside the cylinder[3].

Previous studies have established that the spray properties are influenced by an unusually large number of parameters,including nozzle internal flow effects resulting from cavitations, the jet velocity profile and turbulence at the nozzle exit, and the physical and thermodynamic states of both liquid and gas. Linear stability theory can provide qualitative descriptions of breakup phenomena and predict the existence of various breakup regimes. The regimes are due to the action of dominant forces on the jet, leading to its breakup, and it is important that these forces be identified in order to explain the breakup mechanism in each regimes. Chandrasekhar (1961) took into account the liquid viscosity and the liquid density, which was neglected by Rayleigh, and showed mathe-

matically that the viscosity tends to reduce the breakup rate and increase the drop size. Taylor (1962) showed that the density of the ambient gas has a profound effect on the form of the jet breakup. For a sufficiently large gas inertia force (which is proportional to the gas density) relative to the surface tension force per unit of interfacial area, the jet may generate at the liquid-gas interface droplets with diameters much smaller than its own diameter.[4] Rayleigh (1879) showed that the jet breakup is the consequence of
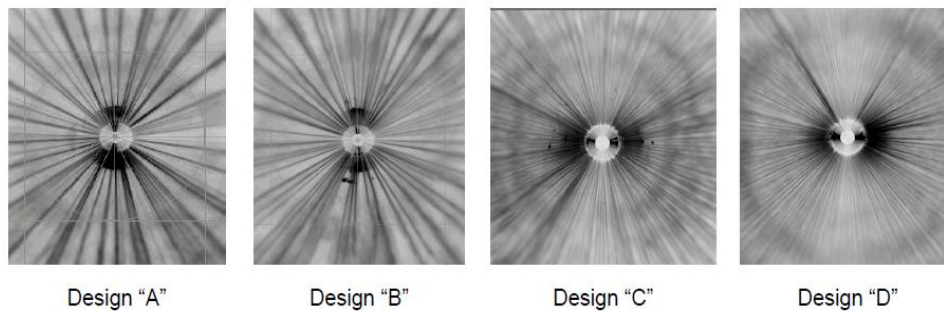

Design "A"   Design "B"   Design "C"   Design "D"

Figure 2.1: In design a & b the spray structure is coarse but in design c & d the spray structure in much finer under the condition of constant pressure of 20 Mpa.[4]

hydrodynamic instability. Neglecting the ambient fluid, the viscosity of the jet liquid, and gravity, he demonstrated that a circular cylindrical liquid jet is unstable with respect to disturbances of wavelengths larger than the jet circumference. Among all unstable disturbances, the jet is most susceptible to disturbances with wavelengths 143.7% of its circumference.

Several experimental studies have been used to study the flow characteristics of sprays from fuel injectors. Zhao and Ladommatos [5] have reviewed a number of optical methods that have been used to study in-cylinder mixture formation for both spark ignition and compression ignition IC engines. Laser based experimental studies are most commonly used to study sprays and mixture formation in IC engines.

Spray atomization and evaporation is a complex phenomenon. The droplet size distribution in a spray can be measured based on angular distribution of elastically scattered radiation. Some of the important laser based techniques are: Laser Rayleigh Scattering (LRS) [19-14]; Spontaneous Raman Scattering (SRS) [6-9]; Laser Induced Fluorescence (LIF) [10-

17]; and Laser Induced Exciplex Fluorescence (LIEF)[18-24].Injector flow characteristics like the shape of the spray, half cone angle and penetration depth can be determined using flow visualization technique that uses Mie scattering from a pulsed laser[24,25,26-29]. In order to achieve the objectives of optimum fuel distribution within the combustion chamber together with high fuel air mixing rate. Flow visualization experiments comprising of shadowgraph/schlieren technique coupled with high speed photography has been used to visualize spray for both gasoline and alcohol/gasoline mixtures. When liquid injections takes place with high relative velocity between the two phases, more complex phenomena needs to be taken into account like turbulence induced breakup, multiple droplet collision in the dense spray region, fluctuations due to cavitation flow inside the injector.Various types of turbulence modeling schemes have been used to model gas phase turbulence and its effect on droplet dispersion including k-ϵ model and its variants[29-42], Large Eddy Simulation and Direct Numerical Simulation[38-44].

Several numerical investigations have to been performed in the past to study droplet evolution and air/fuel mixture formation and is reviewed by Jiang et al.. Spray and atomization can be broadly classified as two phase flow because both the liquid and gas phases need to be resolved. Generally two different approaches are followed to numerically solve two-phase spray problems: (a) Eulerian approach, where the liquid and gas phase, both are traced using continum mechanics in whole flow domain (b) Lagrangian approach, where the paths taken by the droplets or cluster of droplets are considered as particles and are tracked in the whole flow domain.

Most of the spray studies performed previously using Eulerian interface tracking methods were under isothermal conditions[45-47]. However, real operating conditions in an SI engine with Port Fuel Injection (PFI) system is highly non-isothermal. The ambient temperature is several degrees higher than the liquid droplets and vapour liquid equilibrium thermodynamics for gasoline/alcohol blends is very complex. Therefore, liquid jet disintegration and droplet evolution for such blends is strongly dependent on interfacial heat and mass transfer. In the case of port-injected gasoline engines, fuel evaporation in the inlet port is controlled by several factors, including droplet size distribution, surface temperature surface roughness, surface deposits and surface material. For example, in

port-injected engines, only the smallest droplets of less than about 20μm diameter can follow the air stream past an open inlet valve.

However, in practice, a large fraction of the injected fuel have diameters greater than 100μm. These relatively large droplets impinge on various hot surfaces within the engine inlet port, from where they evaporate. The inlet port surface temperature, at intermediate engine loads and speeds, is usually around 40 to 70°C. However, at the back of the inlet valves, temperatures can be much higher and exceed 200°C at high engine loads and speeds. Nowadays it is common practice to target the fuel spray on to the back of the inlet valves where the high surface temperature can enhance fuel evaporation rates. Eceeded substantially the liquid boiling point (e.g. by 50 or 60°C). Leidenfrost evaporation occurred at surface temperatures significantly greater than the liquid boiling point (e.g. by 100°C), and the droplets levitated off the hot surface on to a cushion of vapour.

Agarwal has reviewed in detail biofuel applications for internal combustion engines. He has shown that ethanol addition to gasoline results in better engine performance and efficiency[48]. Parameters like brake power, thermal efficiency, volumetric efficiency, fuel consumption shows an improvement with ethanol addition. Such fuel blends show a decrease in CO and unburned hydrocarbon emissions, with slight increase in CO_2 emission. Niven has also reviewed ethanol/gasoline blends from an environmental and sustainability point of view. They have reviewed use of ethanol/gasoline blends based on[51]:

1. Air pollution emissions

2. Impact on subsurface soils and groundwater

3. Reduction in greenhouse gas emissions

4. Energy efficiency

5. Overall sustainability of ethanol production.

.

Kunimitsu, et al.have developed a model of vapor generation which under non-boiling conditions employs the Reddy's correlations. Under boiling conditions, the model uses empirically generated single plate distillation data at 1 atmosphere pressure to relate fuel

temperature to fraction evaporation. No provisions were made for pressure rise due to vent restrictions. They have indicated that there might be an increase of photochemical smog when ethanol is blended with gasoline at low concentrations. In another review paper, Blottnitz et al.compares several bio-ethanol systems to conventional fuel on a life cycle basis. Some of the important findings of this review were:

- Make ethanol from sugar crops in tropical countries.

- Hydrolysis and fermenting lignocellulosic residues to ethanol.

- Life cycle assessment on grasses as feedstock are insufficient to draw conclusions.

Ethanol can also be blended with diesel fuel, which results in lower particulate emissions. In another study a comparison of ethanol and butanol as oxygenates in gasoline was performed to determine their effect on engine performance. They reported that butanol performed equally well as ethanol from emission and combustion point of view with a decrease in fuel consumption[52].

Mass transfer contributions from each component evaporating into the carrier gas was calculated and source terms were accordingly implemented in the continuity, momentum, energy and species equations. This model was used to study the effect of liquid inlet temperature and composition, exit pressure, temperature and gas composition in counter-current stratified two-phase flow system.

The study of evaporation of a single droplet is necessary for characterizing and understanding the spray vaporization and combustion. There is a large amount of work on study of single droplet evaporation of various kinds liquid fuels. Evaporation behavior of single component fuel droplet has been analytically and experimentally studied under several environments. Some important review papers present the state of the art in single droplet evaporation and combustion [53]. The effects of temperature and pressure on vaporization of single droplet in normal and microgravity have been investigated experimentally[54]. In many applications fuel droplets consist of a mixture of two or more pure liquids. This multicomponent droplet may consist of several species with completely different physical and chemical properties. The degree of volatility, boiling temperature, evaporation latent heat, and heat capacity of each component play an important role

in the interior thermo-fluid dynamics of the droplet. The evaporation characteristics of multicomponent droplet have been analytically and experimentally studied[55].

2.2   Present Work:

As has been explained before, a thorough understanding of the fluid mechanics and mass transfer processes is required to predict the phenomenon of evaporation of fuel droplets. In the present work, an attempt has been made to address these objectives using Computational Fluid Dynamics(CFD). Present study involves, in conjunction with VOF multi phase model to study the evaporation of a single and multi-droplets of binary mixture of iso-octane/ethanol(i.e. E0, E10, E20, E85) under stratified flow conditions within and between the fluid with deforming interface. Source terms arising due to interfacial mass transfer are implemented in the continuity, momentum, energy and species equations.

CFD simulations of two phase stratified flow with 2-D mesh having dimensions of flow-domain as $(400x533)\mu m^2$ were conducted using commercially available software packages ICEM Cfd Package for grid generation and FLUENT(Ansys 12.1), for solving the two phase flow equations. Simulations were done for varying inlet temperature(velocity inlet), varying compositions of binary mixtures, taking in account the effect of gravity over the flow and the results were documented.

To determine evaporation of droplet, evaporation over the liquid surface needs to be modeled. A mass transfer model for binary mixturs has been developed to model evaporation over the liquid surface. As a first step, evaporation of a single component has been simulated. Once the robustness and the accuracy of the model for single component fluids was established(with the help of grid independence study, it has been extended for multi droplet evaporation cases.

The evaporation model was implemented using the user-defined-function (UDF) option available in FLUENT. After implementing the UDF in FLUENT, simulations were performed using ethanol, iso-octane(liquid and vapor) and air as the working fluids. Evaporation rate was determined for Reynold number around 400 (laminar flow case).

Chapter 3

Numerical Procedure

3.1 Multiphase Model

One of the commonly used method to track the free surface flows is the Fixed Grid Eulerian Method. This property is especially advantageous for complex fluid configurations where time-to-time grid reconstruction may be difficult. An example of this method is multi-bubble computation in bubble column reactors [61]. Fixed-grid Eulerian methods do not require a complex iterative strategy, for solving conservation equations in different solution regimes connected through the boundary conditions along the a priori unknown interfaces. This is because different fluids are treated as one with varying properties and discontinuous effects such as surface tension are added as additional volume forces acting in appropriate control volumes. In general, the interface does not coincide with the grid lines. Therefore, for tracking material lines or interfaces, leads to surface or volume tracking techniques. Some of them are described below:

- SEA Method and Enthalpy Models

- FLAIR Method

- Level Set Method

- VOF Method

SEA Method and Enthalpy Models

Closely related to the VOF method are the Enthalpy algorithm [60] and the SEA algorithm [61]. Due to single-valued relationship between temperature and enthalpy, both models are used to simulate solidification and melting processes and at the same time track the involved interfaces solely based on the energy equation. SEA method solves a scalar marker equation and can be extended to the areas of gas-liquid interfaces occurring, for example in casting and molding.

FLAIR Method

In contrast to VOF, FLAIR (Flux Line-segment model for Advection and Interface Reconstruction) method developed by, Ashgriz and Poo [62] is able to reconstruct the interface using a continuous polygon, resulting in a slightly higher precision in interface advection. However, this can only be achieved by defining a large number of geometrical cases including several subcases for each of the independently treated computations of interface slope and curvature.

Level Set Method

Level Set Methods are numerical techniques which can follow the evolution of interfaces, tracking an interface boundary. These interfaces can develop sharp corners, break apart, and merge together. The techniques have a wide range of applications, including problems in fluid mechanics, combustion, manufacturing of computer chips, computer animation, image processing, structure of snowflakes, and the shape of soap bubbles.

Volume of Fluid Model

The VOF model can simulate flow of two or more immiscible fluids by solving a single set of momentum equations and tracking the volume fraction of each of the fluids throughout the domain with a segregated solver having incompressible flow. Typical application includes the prediction of jet breakup, the motion of large bubbles in a liquid, the motion of liquid after a dam break, and the steady or transient tracking of any liquid-gas interface.

VOF (Volume of Fluid) is a volume tracking method. It was developed by Nichols and Hirt [59]. VOF model uses an interface reconstruction algorithm with increased resolution combined with an interface advection method. By using different techniques for solving a scalar marker transport equation, numerical diffusion and interface smearing is controlled. The VOF formulation relies on the fact that two or more fluids (or phase) are not inter-penetrating. For each additional phase, a variable is introduced: the volume fraction of the phase in the computational cell. In each control volume, the volume fractions of all phases sum to unity. The fields for all variable and properties are shared by the phases and represent volume-averaged values, as long as the volume fraction of each of the phase is known at each location. Thus the variables and properties in any given cell are either purely representative of one of the phases, or representative of a mixture of the phases, depending upon the volume fraction values. In other words, if the qth fluid's volume
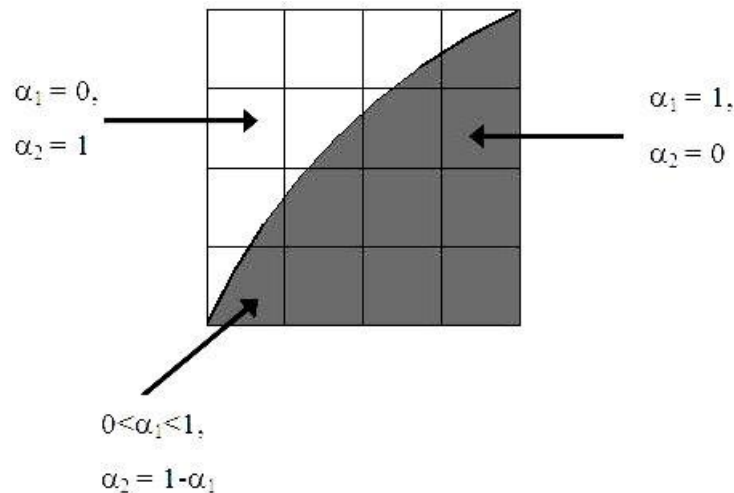
Figure 3.1: Volume fraction of qth fluid in multiphase flow in a computational domain

fraction in the cell is denoted as α_q, then the following three conditions are possible:

$$\alpha_q = 0 \qquad\qquad thecellisempty \qquad\qquad (3.1)$$

25

$$\alpha_q = 1 \qquad\qquad the cell is full \qquad\qquad\qquad (3.2)$$

$$0 < \alpha_q < 1 \qquad cell contains the interface between the fluids \qquad (3.3)$$

Based on the local value of α_q, the appropriate properties and variables will be assigned to each control volume within the domain. The tracking of the interface between the phases is accomplished by the solution of a continuity equation for the volume fraction of multi-phase flow. For the qth phase, this equation has the following form:

$$\frac{\partial \alpha_q}{\partial t} + u_i \frac{\partial \alpha_q}{\partial x_i} = 0 \qquad\qquad (3.4)$$

The volume fraction equation will not be solved for the primary phase; the primary-phase volume fraction will be computed based on the following constraint:

$$\sum_{q-1}^{n} \alpha_q = 1 \qquad\qquad (3.5)$$

The properties appearing in the transport equations are determined by the presence of the component phase in each control volume. In a two-phase system, for example, if the phases are represented by the subscripts 1 and 2, and if the volume fraction of the second of these is being tracked, the density in each cell is given by

$$\rho = \alpha_2 \rho_2 + (1 - \alpha_2) \rho_1 \qquad\qquad (3.6)$$

A single momentum equation is solved throughout the computational domain and the resulting velocity is shared among the phases. The momentum equation is solved using the properties, which are calculated from the volume fractions of all phases. The momentum

equation has the form:

$$\frac{\partial \rho u_i}{\partial t} + \frac{\partial \rho u_i u_j}{\partial x_j} = -\frac{\partial p}{\partial x_i} + \frac{\partial}{\partial x_i}\mu(\frac{\partial u_i}{\partial x_j} + \frac{\partial u_j}{\partial x_i}) + \rho g_i + F_j \qquad (3.7)$$

The source term F_j represents body force due surface tension. Surface tension arises as a result of unbalanced intermolecular attractive forces at the surface. For example, consider an air bubble inside liquid water or the concave free-surface of water flowing in a pipe. Within the air bubble or underneath the free-surface of the liquid, the net forces on a molecule is zero the spatially uniform distribution of the attractive forces. However at the surface, the net force is radially inward for the bubble and radially outward for the free-surface liquid in the pipe. The resultant radial force causes to contract the surface of the bubble or flatten the free-surface of the liquid in the pipe, therefore increasing the pressure at the surface. Hence, surface tension is a force that acts only at the surface to maintain equilibrium for such cases.

In ANSYS FLUENT surface tension is modeled by using the continuum surface force (CSF) model by Brackbill et al. [58]. With this model, the addition of surface tension to the VOF calculation results in the source term F_j in the momentum equation. To understand the origin of the source term, consider the special case where surface tension is constant along the surface, and only the forces along the normal to the surface are considered. It can be shown that the pressure drop across the surface depends upon the surface tension coefficient and the surface curvature as measured by the two radii in the orthogonal directions, R1 and R2:

$$p_1 - p_2 = \zeta[\frac{1}{R_1} + \frac{1}{R_2}] \qquad (3.8)$$

where, p_1 and p_2 are the pressures in the two fluids on either side of the interface.

In FLUENT, the surface formulation using CSF model can be used only for two phase system. The surface curvature is computed from the local gradients of the surface normal to the interface. If the surface normal $\vec{n}$, defined as the gradient of α_2, the volume fraction

of the secondary phase then,

$$\vec{n} = \nabla\alpha_2 \tag{3.9}$$

The curvature, κ, is defined in terms of the divergence of the unit normal, $\vec{n}$

$$\kappa = \nabla.\hat{n} \tag{3.10}$$

where

$$\hat{n} = \frac{\vec{n}}{|n|} \tag{3.11}$$

Surface tension can be written in terms of pressure jump across the interface. The force at the surface can be expressed as a volume force using the divergence theorem. It is this volume force that is the source term which is added to the momentum equation. It has the form:

$$F_j(\kappa) = 2\zeta\kappa(\kappa)\alpha_2\nabla\alpha_2 \tag{3.12}$$

The source term is added only to one side of the interface, i.e. the side on which volume fraction calculations are done.

As control volume approach is used in FLUENT, the convection and diffusion fluxes through the control volume faces are computed and balanced with the source terms within the control volume itself. There are four methods to determine the surface fluxes in VOF method: Geometric Reconstruction, Donor-Acceptor, Euler Explicit and Implicit methods. For the present work, geometric reconstruction has been used because it gives the sharpest interface between two phases. Fig.[3.2] shows the actual interface shape and Fig.[3.3] the interface represented by geometric reconstruction method. Geometric reconstruction method can only be used for a time dependent solution.

The geometric reconstruction scheme represents the interface between the fluids using a piecewise-linear approach. Geometric reconstruction method has been extended to unstructured grid from the work of Youngs [56]. It assumes that the interface between the two fluids has a linear slope within each cell and uses this linear shape for the calculation of the advection of fluid through the cell faces.

Geometric reconstruction scheme works in three steps. The first step in this scheme is

28
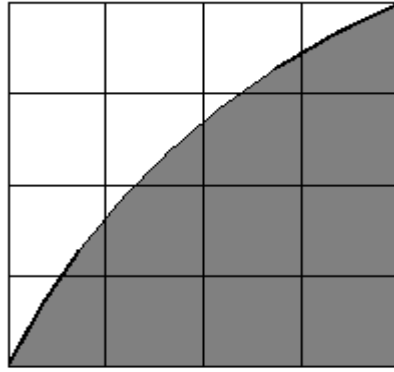
Figure 3.2: Actual Interface Shape
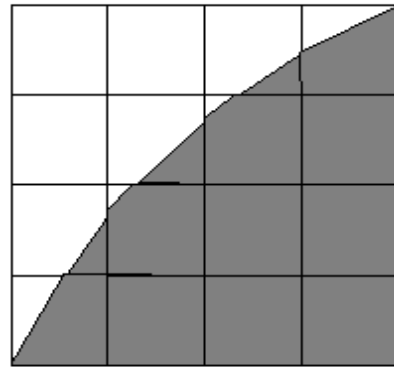
Figure 3.3: Interface Shape after geometric re-construction

calculating the position of the linear interface relative to the center of each partially filled cell, based on the information about the volume fraction and its derivatives in a cell. The second step is calculating the advecting amount of the fluid through each face using the computed linear interface representation and information about the normal and tangential velocity distribution on the face. The third step is calculating the volume fraction in each cell using the balance of fluxes calculated during the previous time step. The governing equations used in this analysis are mentioned as follows:

Governing Equation

Energy Equation :

$$\frac{\partial}{\partial t}(\rho E) + \nabla.[u(\rho E + p)] = \nabla.(k_{eff}\nabla T - \sum_i h^i j^i) + S_e \qquad (3.13)$$

Energy, E and temperature, T are mass-averaged variables and written as:

$$E = \frac{\sum_{q=1}^n \alpha_q \rho_q E_q}{\sum_{q=1}^n \alpha_q \rho_q} \qquad (3.14)$$

Species Equation :

Two set of species equation has been solved in gaseous phase where as for liquid phase single equation has been solved as liquid phase is binary component mixture of ethanol and iso-octane only. The species equation is described as

Species equation is solved under VOF model and expressed as :

$$\frac{\partial}{\partial t}(\rho_q \alpha_q y_q^i) + \nabla.(\rho_q \alpha_q u y_q^i) = -\nabla.(\alpha_q \vec{j_q^i}) + S^i \qquad (3.15)$$

where the diffusion flux $\vec{j^i}$ appears in above equations is given as :

$$\vec{j^i} = -\rho D_{eff}^i \nabla y^i \qquad (3.16)$$

Interface Conditions-Evaporation Calculation

In this study mass flux term was obtained directly from normal component of species gradient at the interface. Evaporation rate per unit volume can be expressed as :

$$m_i''' = \frac{\dot{m}_i'}{V_{cell}} = -\rho_g D_{eff}^i \nabla y^i.\frac{A}{V_{cell}} \qquad (3.17)$$

where A is defined as

$$A = V_{cell}\nabla \alpha_g \qquad (3.18)$$

Combining both the above mentioned equations 3.17 and 3.18, Evaporation rate can be expressed as

$$m_i''' = -\rho_g D_{eff}^i \nabla y^i . \nabla \alpha_g \tag{3.19}$$

Source terms used in governing equations, is due to evaporation from the surface of liquid phase are described in section below.

VOF equation:

For liquid and gas phase, source term is

$$S_{\alpha l} = -\sum_{i-1}^{N} m''' \tag{3.20}$$

$$S_{\alpha g} = \sum_{i-1}^{N} m''' \tag{3.21}$$

Momentum equation:

As due to Evaporation, the momentum is lost in liquid phase and hence gained in gas . Therefore a volume fraction average momentum equation source term is expressed

$$S_m = (1 - 2\alpha_l) \sum_{i=1}^{N} m''' u \tag{3.22}$$

Energy equation:

$$S_e = -\rho \sum_{i=1}^{N} \frac{m_i'''}{\rho_l} h_{fg}^i \tag{3.23}$$

Species equation:

Source term for gas phase species equation is expressed as

$$S_i = m_i''' \tag{3.24}$$

31

and only ethanol is tracked in liquid phase w.r.t iso-octane, hence evaporation rate of ethanol relative to iso-octane has been applied as source term for liquid phase and expressed as:

$$S^i = m'''_{C_2H_5OH} - m_{C_8H_{18}} \tag{3.25}$$

Interface Mass Fraction: The binary mixture of ethanol and iso-octane is a non-ideal mixture due to high polarity of ethanol molecules. Therefore, vapour pressure of the liquid phase depends upon the composition of liquid. The interface mass fraction is calculated from

$$y^i = \frac{x^i M^i}{\sum_{i=1}^{N} x^i M^i} \tag{3.26}$$

where activation co-efficient has been calculated using UNIFAC method[where interface mole fraction is given as

$$x^i = \eta \frac{\gamma^i X^i P_v a p^i}{P} \tag{3.27}$$

3.2   Computational Model

ANSYS FLUENT uses control-volume based technique to convert the governing equations into algebraic equations, which can be solved numerically. Control volume technique consists of integrating the governing equations about each control volume, yielding discrete equations that conserve each quantity on a control-volume basis. A detailed discussion on the control volume technique is given in references [57, 58]. The control-volume based technique consists of the following steps:

- Division of the domain into discrete control volumes using a computational grid.

- Integration of the governing equations on the individual control volumes to construct algebraic equations for the discrete dependent variables such as velocities, pressure, temperature, and conserved scalars.

- Linearization of the discretized equations and solution of the resultant linear equation system to yield updated values of the dependent variables.

As the governing equations are non-linear and coupled, several iterations are required to obtain a converged solution. A segregated solver, where the governing equations are solved sequentially, was used to perform the iterations. This is due to the restriction that FLUENT imposes on the choice of the solver with VOF multiphase model. Using this approach, the governing equations are solved sequentially. Each iteration consists of the steps outlined below:

- Fluid properties are updated, based on the current solution.(If the calculation has just begun, the fluid properties will be updated based on the initialized solution).

- The u, v and w momentum equations are each solved in turn using current values for pressure and face mass fluxes, in order to update the velocity field.

- Since the velocities obtained in Step 1 may not satisfy the continuity equation locally, an equation for the pressure correction is derived from the continuity equation and the linearized momentum equations. This pressure correction equation is then solved to obtain the necessary corrections to the pressure and velocity fields and the face mass fluxes such that continuity is satisfied.

- Appropriate scalar equations such as turbulence, species, etc. are solved using the previously updated values of the other variables.

- A check for convergence of the equation set is made.

These steps are continued till convergence is achieved. An overview of the segregated solver is shown in Fig.[3.4].

Only implicit method of linearization can be used with segregated solver. In implicit linearization technique, the unknown value in each cell is computed using a relation that includes both existing and unknown values from neighboring cells. Therefore each unknown will appear in more than one equation in the system, and these equations must be solved simultaneously to give the unknown quantities.

To model the convection term in the governing equations, upwind scheme was used. FLUENT provides the choice between first-order and second order upwind schemes. When first-order accuracy is desired, quantities at cell faces are determined by assuming that the
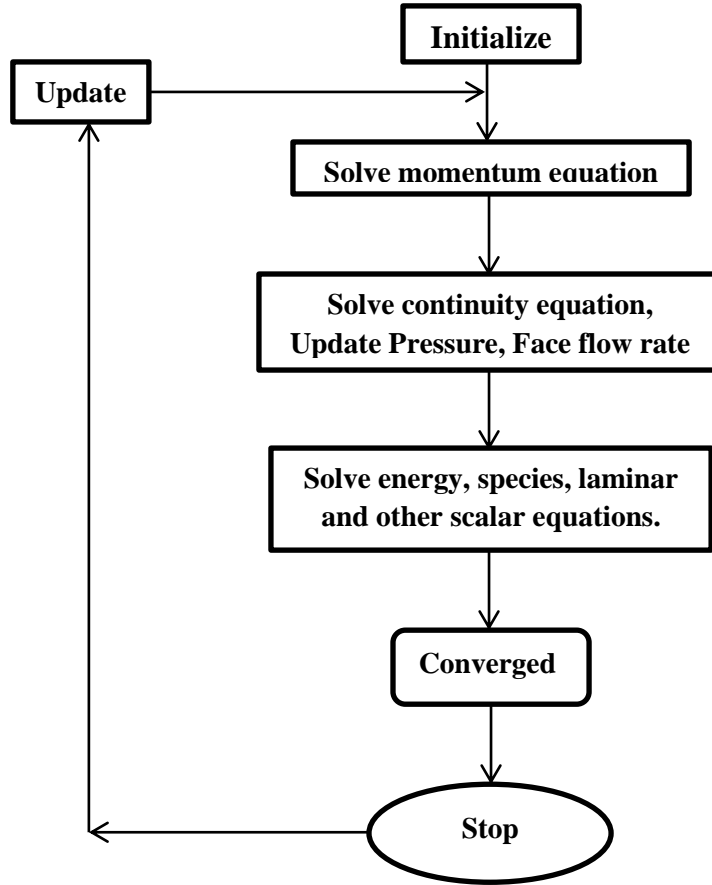
Figure 3.4: Overview of segregated solver

cell-center values of any field variable represent a cell-average value and hold throughout the entire cell; the face quantities are identical to the cell quantities. In second order upwind scheme, quantities at cell faces are computed using a multidimensional linear reconstruction approach. In this approach, higher-order accuracy is achieved at cell faces through a Taylor series expansion of the cell-centered solution about the cell centroid. Thus when second-order upwinding is selected, the face value f is computed using the following expression:

$$\phi_f = \phi + \nabla\phi \cdot \Delta s \tag{3.28}$$

where ϕ and $\nabla\phi$ is the cell centered value and its gradient in the upstream cell, respectively. Δs is the displacement vector from the upstream cell centroid to the face centroid.

The gradient $\nabla\phi$ is computed using the divergence theorem, which in discretized form is written as:

$$\nabla\phi = \frac{1}{v}\sum_f^N \tilde{\phi}A \qquad (3.29)$$

Here the face values $\tilde{\phi}$ are computed by averaging ϕ from two cells adjacent to the face. The generalized discretization equation for scalar transport equations at cell at point p can be written as:

$$a_p = \sum_{nb} a_{nb}\phi_{nb} + b \qquad (3.30)$$

where a_p and a_{nb} are the linearized coefficients of and the neighboring nb, respectively. Other than at the boundaries, the number of neighbors for each cell depends on the grid topology, but will typically equal the number of faces enclosing the cell. Similar equations can be written for all cells and solved iteratively.

The discretization equation for the momentum equation is written in a slightly different manner and is shown in Equation 3.31:

$$a_p\phi = \sum_{nb} a_{nb}u_{nb} + \sum P_f \cdot \hat{i}A + b \qquad (3.31)$$

If the pressure field is known, then Equation 3.31 can be solved like any other scalar equation. But, the pressure field is not known a priori and is part of the solution. The pressure field is indirectly known from the continuity equation. Therefore, an algorithm is required that would calculate the pressure field and the velocity profile iteratively. The most commonly used algorithm is SIMPLE [57] and its variants. For the present work SIMPLEC [58] algorithm is used to achieve a faster convergence than SIMPLE algorithm.

Evaporation model is implemented in ANSYS FLUENT 12.1 by using the user defined function (UDF) option. Using UDF, the user can incorporate user specific models in FLUENT. C language was used to write the code for UDF.

Chapter 4

Results and Discussions

As defined earlier[Chap.3], due to high polarity of ethanol molecule, ethanol/iso-octane mixture is refers to be a non-ideal mixture and vapor pressure strongly depends upon the composition of the liquid. In this study, heat and mass transfer is taken in account. The gas phase is tertiary mixture of ethanol, iso-octane and air and the liquid phase is a binary mixture of ethanol and iso-octane. The thermo-physical properties of all species in gas phase as well as in liquid phase are given in Table 4.1 & Table 4.2 for ethanol and Iso-Octane used in this study. The Molecular weight (M^i) of Iso-Octane is 114.231 and that of Ethanol as 46.069. For Ethanol, the fluid properties are :

Table 4.1: Iso-Octane Fluid Properties

Properties	Iso-Octane(liquid)	Iso-Octane(vapor)
Density(ρ)	695.5 Kg/m^3	4.729 Kg/m^3
Thermal Conductivity(k)	0.0995 W/mk	0.0117 W/mk
Specific Heat(C_p)	2037 J/Kg K	1006 J/Kg K
Viscosity(μ)	4.55e-04 Pa.s	0.593e-05 Pa.s

Table 4.2: Ethanol Fluid Properties

Properties	Ethanol(liquid)	Ethanol(vapor)
Density(ρ)	813 Kg/m^3	1.907 Kg/m^3
Thermal Conductivity(k)	0.182 W/mk	0.0154 W/mk
Specific Heat(C_p)	2470 J/Kg K	1006 J/Kg K
Viscosity(μ)	1.233e-03 Pa.s	8.5753e-05 Pa.s

4.1 Geometry and Grid Generation

In the present CFD work, the geometry and grid was generated using ICEM CFD. It can be very conveniently used to generate two or three dimensional geometries. It can be run interactively to generate structured as well as unstructured grids and the resultant grid can be interactively viewed and optimized for the geometry and the flow problem in consideration. Several parameters can be summoned while generating the grid to determine whether the grid has been optimized.
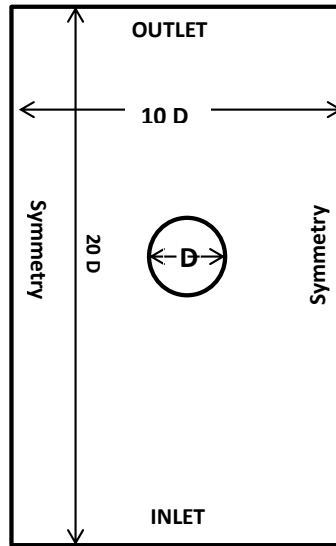
Figure 4.1: Mesh(600x500 m^2)

2D Grid Geometry is created dimension $(400\text{x}533.36)\mu m^2$ with finer meshing keeping in mind the aspect ratio for the grids must be same so as to proceed with mesh optimization.Initial base case is modeled with inlet conditions as Velocity inlet V_{in}=30 m/s having temperature T_{in}=400 K, outlet as Pressure outlet and side walls as symmetry and droplet temperature T_d=300 K. Droplet having diameter (D=20μm) is taken at the center of the grid for base case simulation. Interface mole fraction for ethanol/iso-octane droplet is taken as 0.2. A Uniform grid was created to simulate flow in flow domain.

4.2 Grid Independence study

When solution no longer changes with further grid refinement, then solution is termed as a "grid-independent" solution. Here we are concentrating on the following parameters mentioned below

- Evaporation rate for ethanol and iso-octane is calculated from User Define Memory

  Mass of ethanol and iso-octane is calculated by taking volume integral of equation 3.19 that gives evaporation rate per unit volume and then again integrate that value with respect to time using Trapezoidal Method(Iterative method)and hence mass values has been calculated.

- Average Interfacial Temperature at interface of 0.2 and 0.5 can be compute from surface integral (mass weighted average value).

- Latent Heat can be obtained by performing a volume integeral of equation 3.23.

Meshes are created with help of ICEM Cfd package. The specifications of meshes and results are shown below in the table as

Table 4.3: Mass, Volume and Latent Heat Results

Mesh	M_Ethanol(Kg)	M_Iso-octane(Kg)	Latent_Heat	Vol_Liq(m^3)
180×216	3.11714E-10	3.76245E-10	-2.75344E-05	3.01E-10
250×300	4.07381E-10	5.04523E-10	-3.58371E-05	3.05E-10
355×426	4.92E-10	6.24193E-10	-4.19414E-05	3.10E-10
500×600	5.65049E-10	7.40881E-10	-4.67333E-05	3.10E-10
700×840	6.34206E-10	8.52E-10	-5.10616E-05	3.13E-10
900×1080	6.808E-10	9.32E-10	-5.40491E-05	3.10E-10

Here in above Table.[4.3], mesh size is defined as 180×216 which specifies the number of grid elements along x-axis and y-axis on the scale of $(400 \times 533)\mu m^2$ i.e. grid size along x-axis, y-axis taken as $\Delta X = 3.33\mu m$, $\Delta Y = 2.314\mu m$. Here we are refereing iso-octane instead of gasoline because presently most of the engines are configured with this fuel and moreover it is a pure form of fuel where as gasoline is a complex mixture and study on complex mixtures is much complex as compared to pure form of fuel. However, due to

39

high octane rating of ehtanol/iso-octane as compared to gasoline, these fuels have high antiknocking capacity.

Table 4.4: Results For Interfacial Temperature

Mesh	Temp_interphase_0.2	Temp_interphase_0.5
180×216	310.723	302.783
250×300	306.217	302.979
355×426	307.751	302.984
500×600	306.486	302.740
700×840	306.949	300.89
900×1080	304.642	302.70

Table 4.5: Grid Independance Percentage (%) Change in Mass and Latent Heat values

Mesh	M_ethanol(Kg)	M_iso-octane(Kg)	% Change_Latent Heat
180×216-250×300	30.69%	34.09%	30.15%
250×300-355×426	20.74%	23.72%	17.03%
355×426-500×600	14.88%	18.69%	11.43%
500×600-700×840	**12.24%**	**15.04%**	**9.26%**
700×840-900×1080	7.35%	9.29%	5.85%

Here in the above Table.[4.5], the percentage change in the properties for last and second last row is in between 0-7%. Hence solution is independent here for the grid size. So we will proceed with mesh having grid size dimensions (700×840). Here the grid size for the mesh is about 6 lakhs and after scaling the co-ordinates the elemental grid size approaches the value around 11-12 lakhs. Depending upon the capacity of our high performance computers, to run the simulations for time step 10^-8, the simulations will be executed completely within the time span of 4 to 5 days, and consume lot of time and cost. So keeping in mind about these two factors, we will proceed further toward the test cases with Mesh size $(400×533)\mu m^2$ with grid size along x- and y- coordinates as (500×960) having size around 5 lakhs and hence it will consume less time and cost too. After achieving the Grid Independence, the final mesh for the upcoming Single and Multidroplet Evaporation has been selected, having dimensions as $(400×533)\mu m^2$ and with grid elemental size of (500×950). Next is to, proceed with Single Droplet Evaporation, Test cases.

4.3 Single Droplet Evaporation: Test Cases

In this section, 4 test cases has been executed for ethanol composition i.e.E0, E10, E20 and E85 with varying Temperature at inlet keeping the droplet temperature(T_D=300 K). Simulations has been performed for the time step of 10^{-8}sec. In the evaporation model we are concentrating on the following factors:

1. Surface to Volume Ratio

2. Volume of droplet(m^3)

3. Evaporation Rate (kg/m^3 sec)

4. Temperature at interface 0.2(K)

5. Latent Heat(KJ/Kg)

4.3.1 Test Case 1

At **Inlet Temperaure=400K** In this case, inlet temperature is taken as 400K with droplet at the center of flow domain.
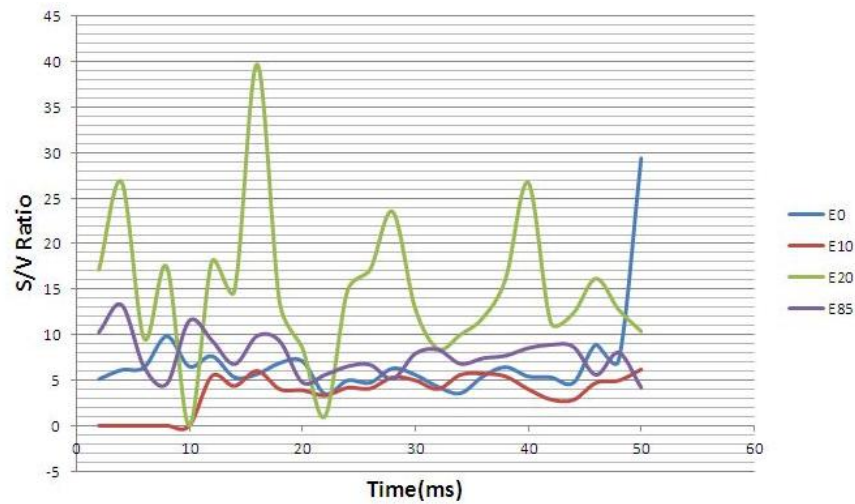
Figure 4.2: Test Case 1: Surface to Volume Ratio

From the above Fig.[4.2] it shows that shape of the droplet is distorted from its initial circular profile. This implies that drag force experienced by droplet is greater due to

41

non-circular profile. Initially fluctuations in surface to volume ratio is more but reduces after certain interval of time.
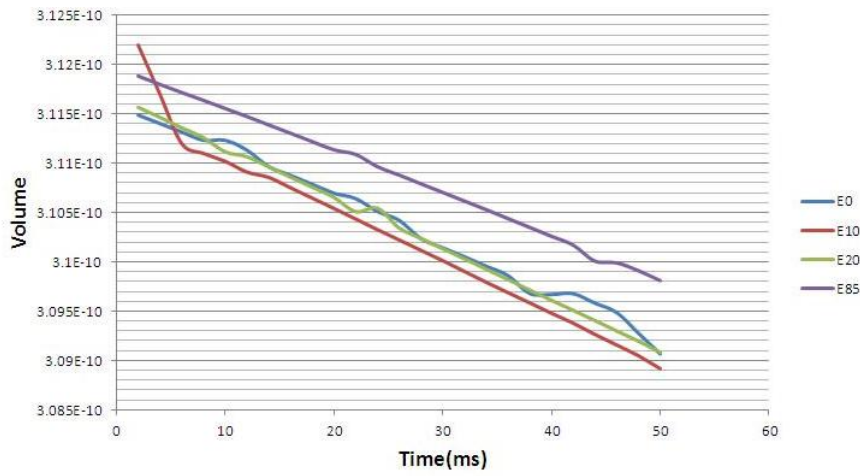
Figure 4.3: Test Case 1: Volume v/s Time

Here in the Fig.[4.3], volume of droplet is analyzed. It shows, Volume in case of E10 is reduced at much faster rate as compared to E0, E10, E85 from its initial time step to final time step because as evaporation occurs the liquid get evaporate into vapors and hence volume get reduced.
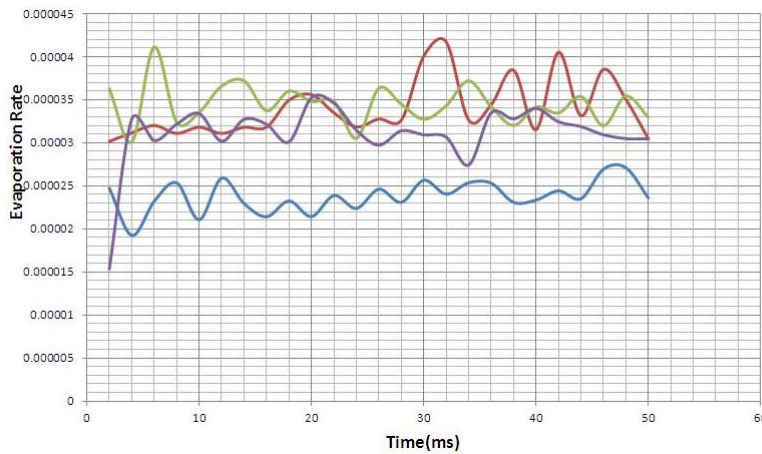
Figure 4.4: Test Case 1: Evaporation rate v/s Time

From the Fig.[4.4], E10 composition of fuels evaporates at higher rate as compared to other compositions, however E0 evaporates slowly at inlet temperature of 400K.
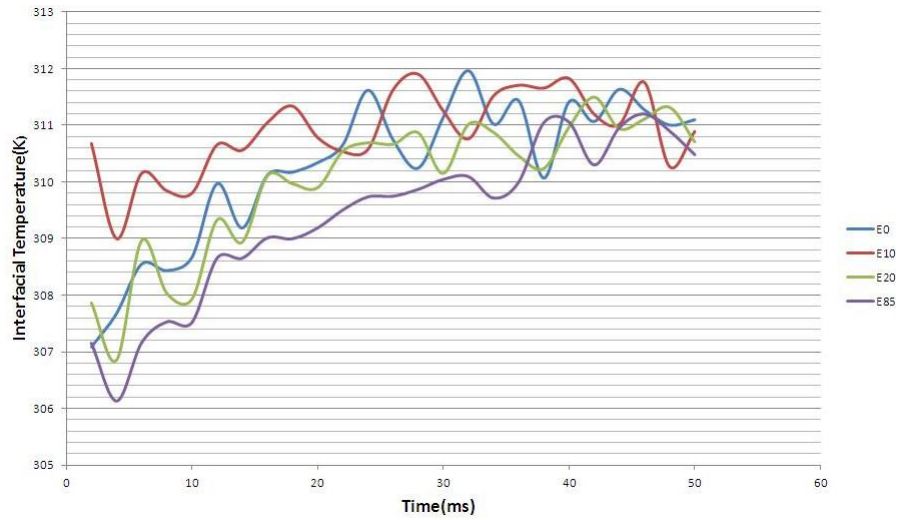
Figure 4.5: Test Case 1: Interfacial Temperature v/s Time

Here From the Fig.[4.5], Temperature for E10, at interface value of 0.2 ethanol/iso-octane interface is more as compared to E0, E20 and E85.
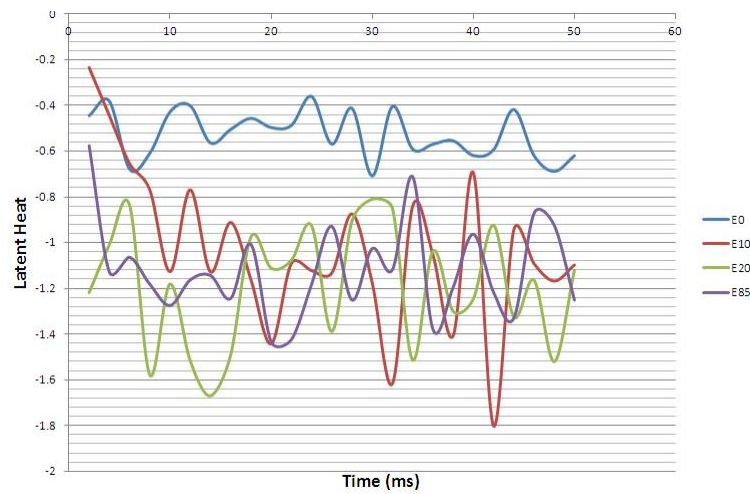
Figure 4.6: Test Case 1: Latent Heat v/s Time

Latent heat is the heat released or absorbed during a change of state that occurs without a change in temperature.In Fig.[4.6] phase transition in case of E0 is more however initially it is higher for E10 composition.

4.3.2 Test Case 2

At **Inlet Temperaure=500K** In this case, inlet temperature is taken as 500K with droplet at the center of flow domain.
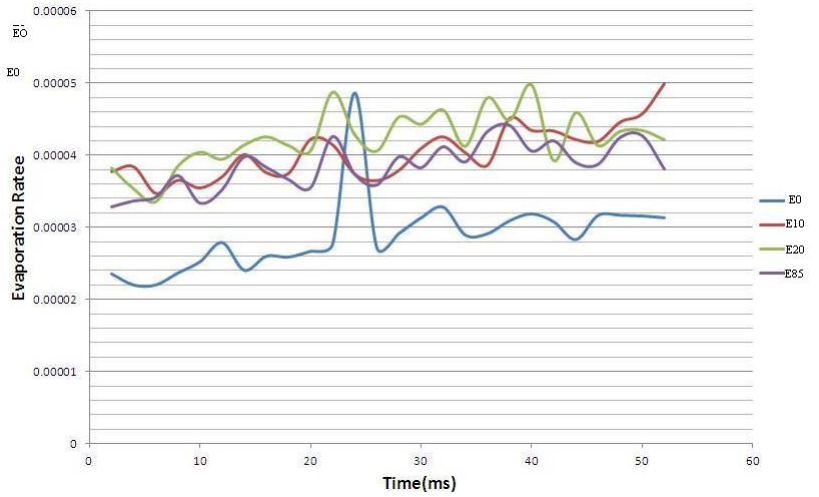
Figure 4.7: Test Case 2: Evaporation v/s Time

In the above Fig.[4.7] for evaporation v/s time, the evaporation rate for E10 is higher as compared to others whereas for E0, its lower.
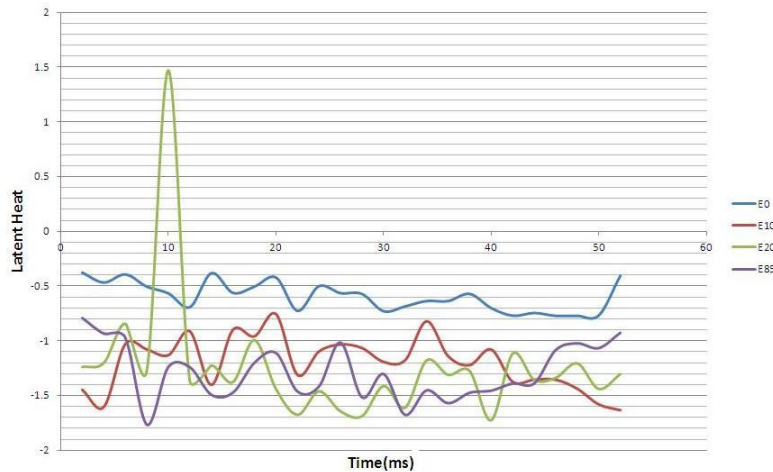
Figure 4.8: Test Case 2: Latent Heat w.r.t Time

In Fig.[4.8], Phase transition in case of E10 is maximum in this case. The negative value of latent heat implies, the evaporating cooling effect.

44
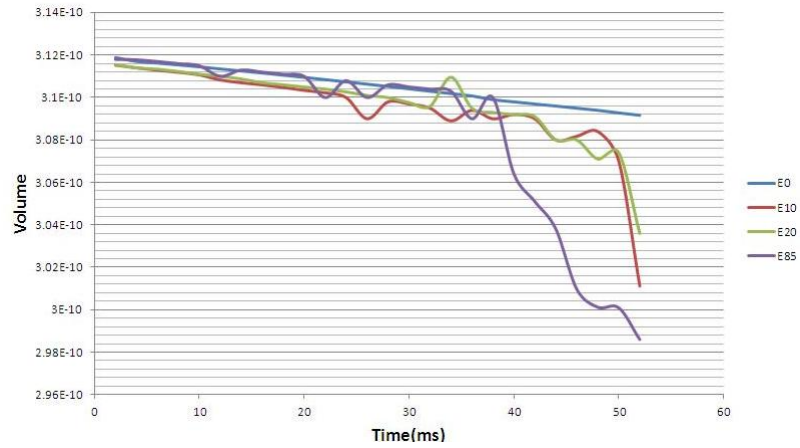
Figure 4.9: Test Case 2: Volume v/s Time

In the figure Fig.[4.9], Volume for E85 Composition get decreased at much faster rate as compared to other compositions. Here E20 and E85 composition, initially have same decrement in volume but after some time interval the volume get reduced in similar manner.
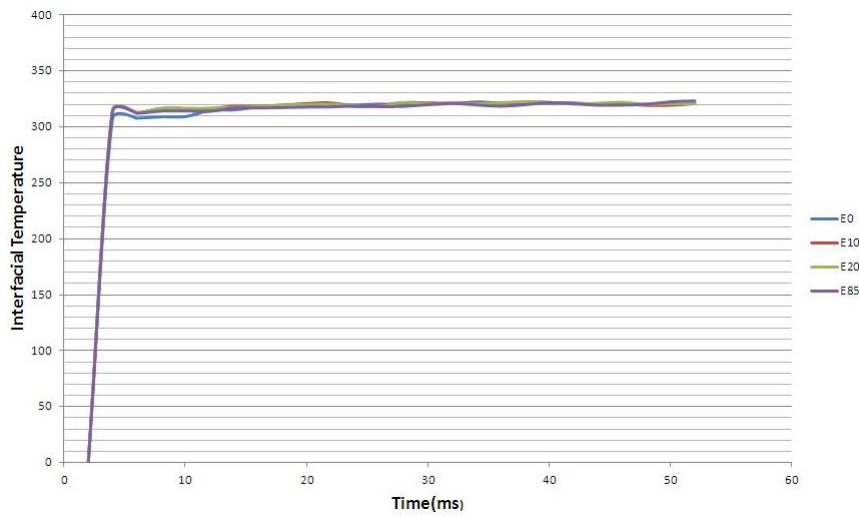
Figure 4.10: Test Case 2: Interfacial Temperature v/s Time

In Fig.[4.10], the interfacial temperature is almost same for all the compositions and increases linearly i.e. for E0, E10, E20, E85.
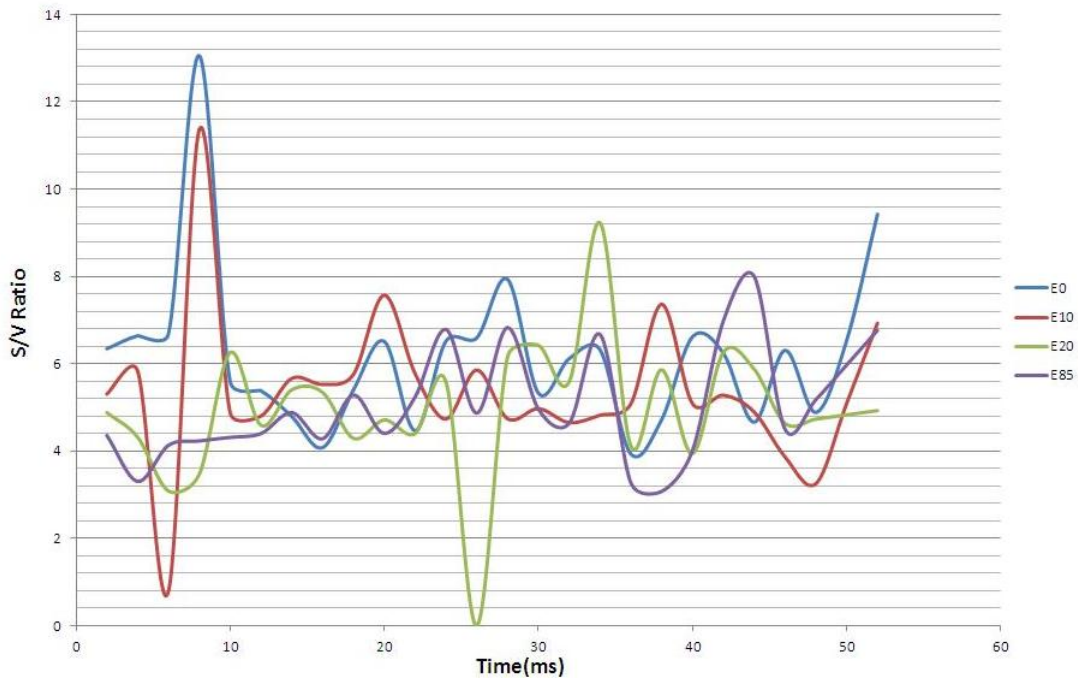
Figure 4.11: Test Case 2: Surface To Volume Ratio v/s Time

From the Fig.[4.11] we can see that E0 droplet has more surface to volume ratio , and in case of E10 initially the surface to Volume ration get some rise and then suddenly decreased and then again rise. This fluctuations in surface to volume ratio occurs due to the forces that are acting onto the droplet in the flow domain. The surface area sometimes increases and sometime reduced to some extent depending upon the shape of the droplet.

4.3.3   Test Case 3

At **Inlet Temperaure=600K**

In this case, inlet temperature is taken as 600K with droplet initially at the center of flow domain. Here in this study case, great effect on the evaporation behavior of E10 composition of iso/octane droplet has been seen which are described from the plots.
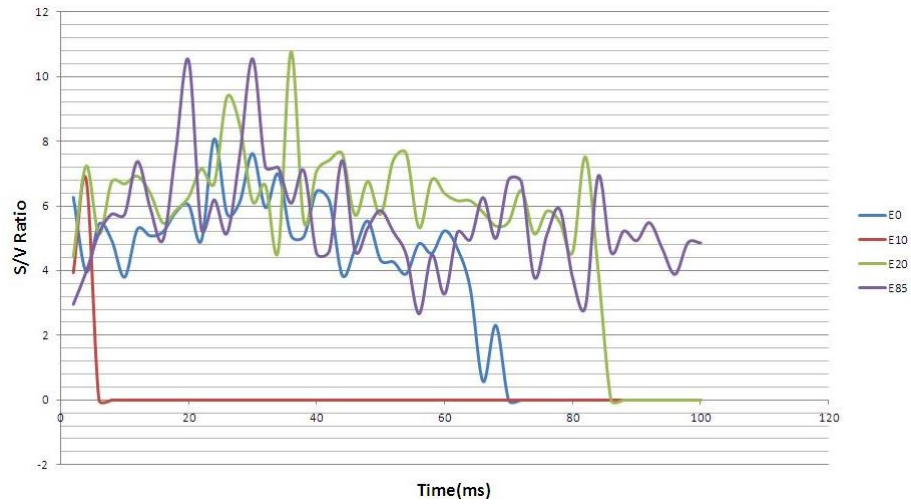
Figure 4.12: Test Case 3: Surface to Volume ratio

In Fig.[4.12], The surface to volume ratio for E0, E20, E85, fluctuates similarly to the above cases but in case of E10 here it shows rapid change in surface to volume ratio. Near about 5-10 ms the droplet get evaporated and hence surface to volume ratio diminish in this case at earlier stage as compared to other compositions.
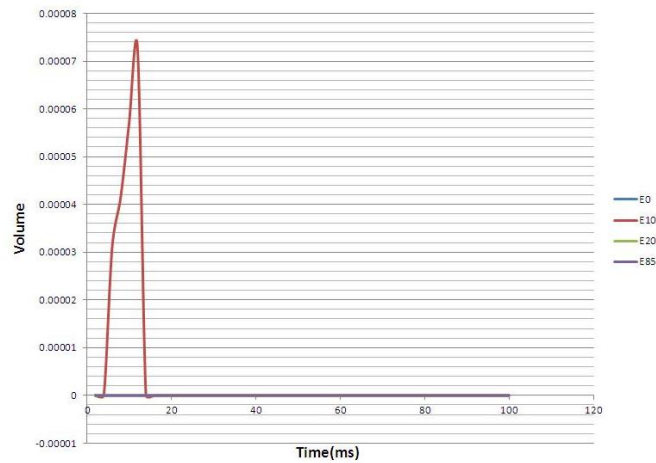
Figure 4.13: Test Case 3: Volume v/s Time

In Fig.[4.13], as mentioned above in surface to volume plot, E10 the droplet spread firsts and then it goes out of the flow domain and hence here volume reduces sharply at the same time. Where as rest three of the cases has been simulated at same frequency w.r.t each other and moves up-to 80 ms.
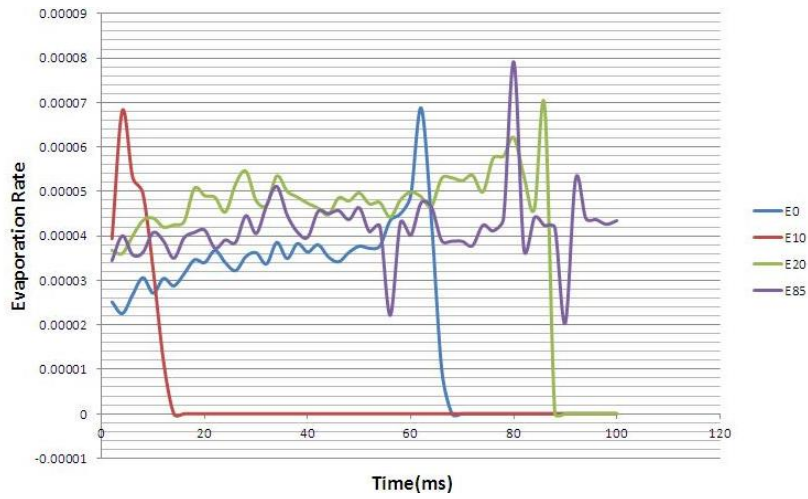
Figure 4.14: Test Case 3: Evaporation Rate v/s Time
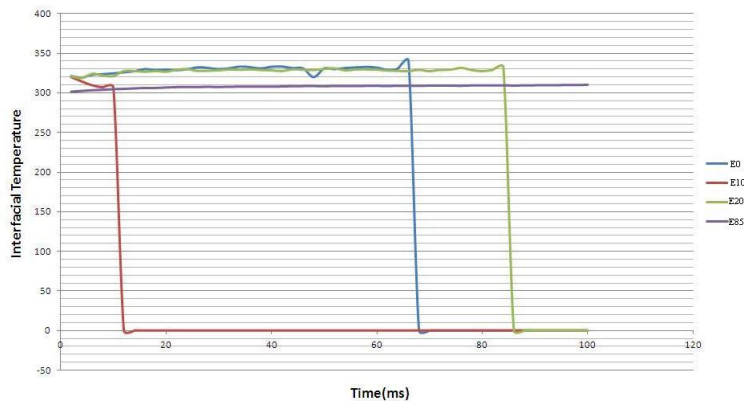
Figure 4.15: Test Case 3: Interfacial Temperature v/s Time
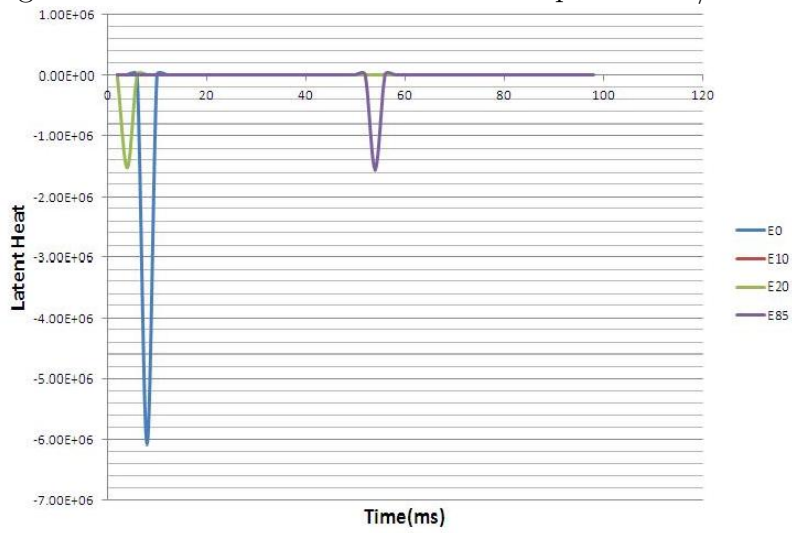
Figure 4.16: Test Case 3: Latent Heat v/s Time

48

4.3.4 Test Case 4

At **Inlet Temperaure=700K**

In this case, inlet temperature is taken as 700K with droplet initially at the center of flow domain.
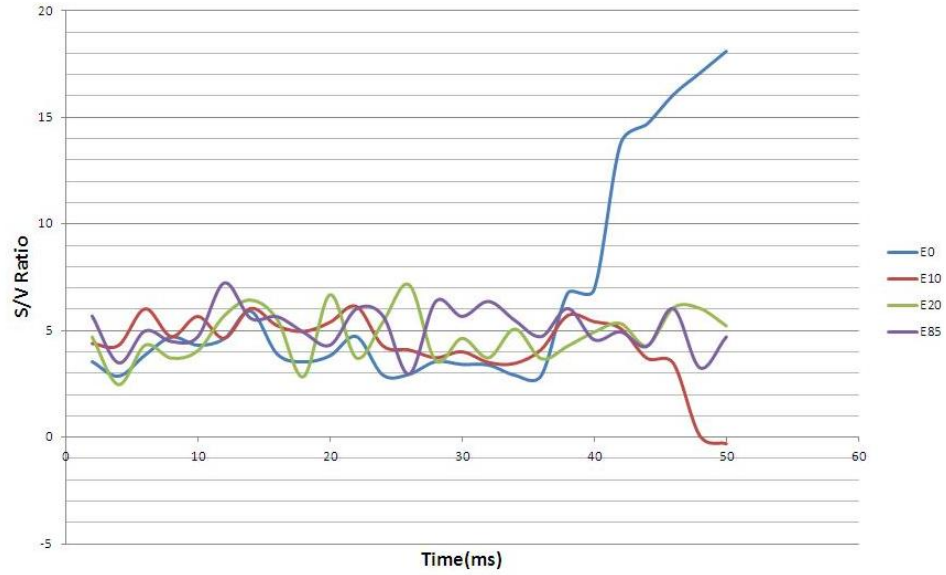
Figure 4.17: Test Case 4: Surface to Volume Ratio v/s Time
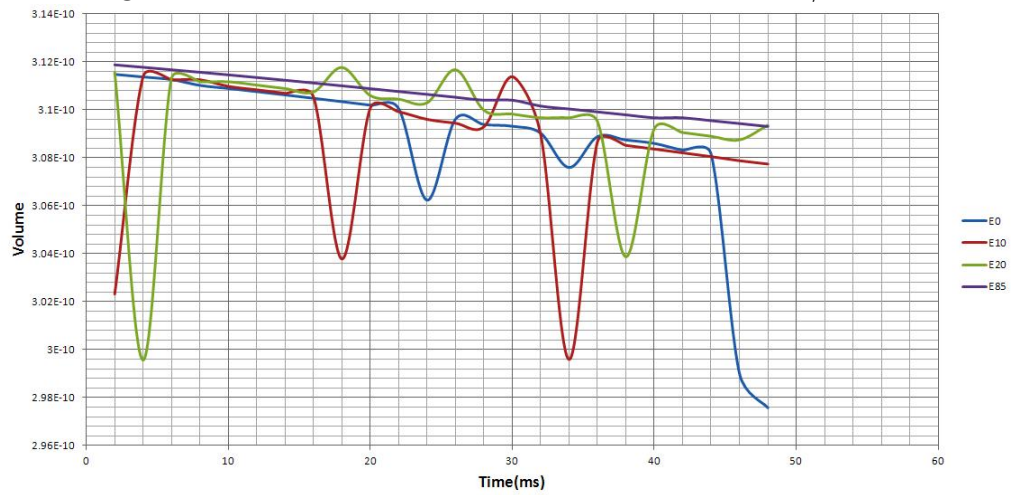
Figure 4.18: Test Case 4: Volume v/s Time
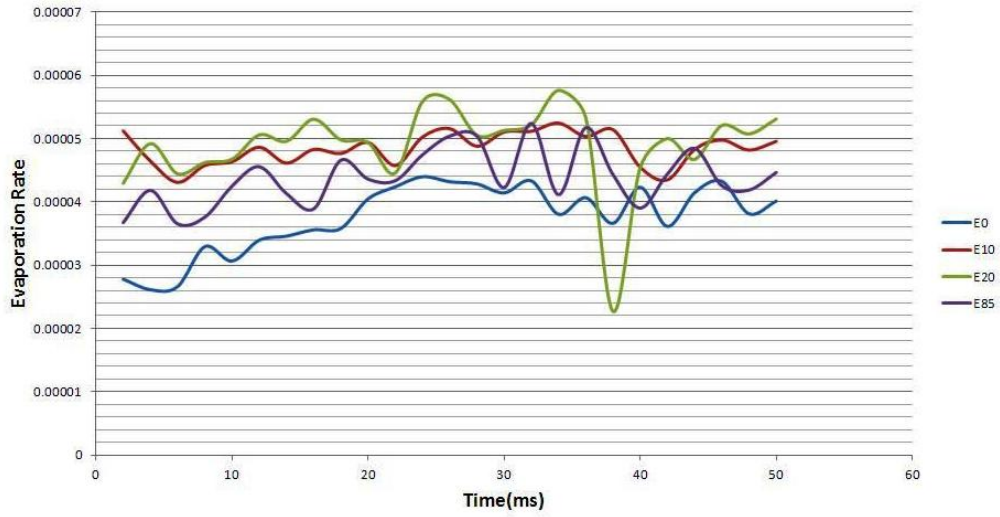
Figure 4.19: Test Case 4: Evaporation Rate v/s Time
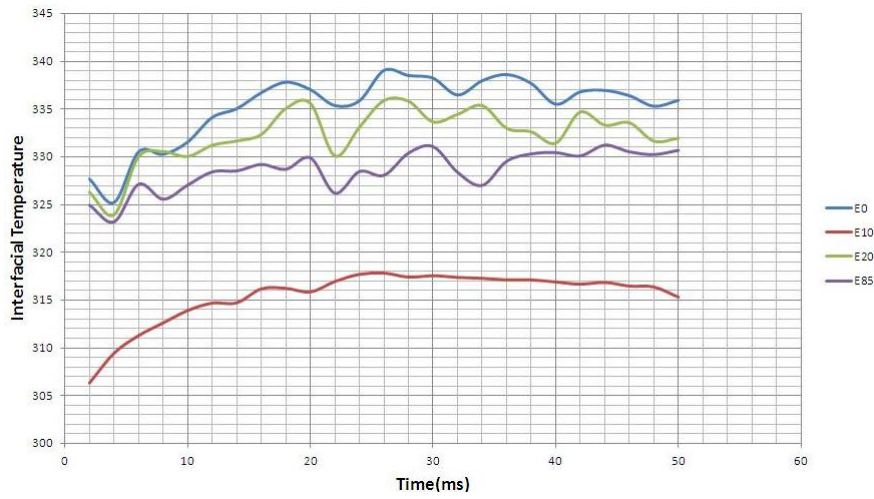
Figure 4.20: Interfacial Temperature v/s Time
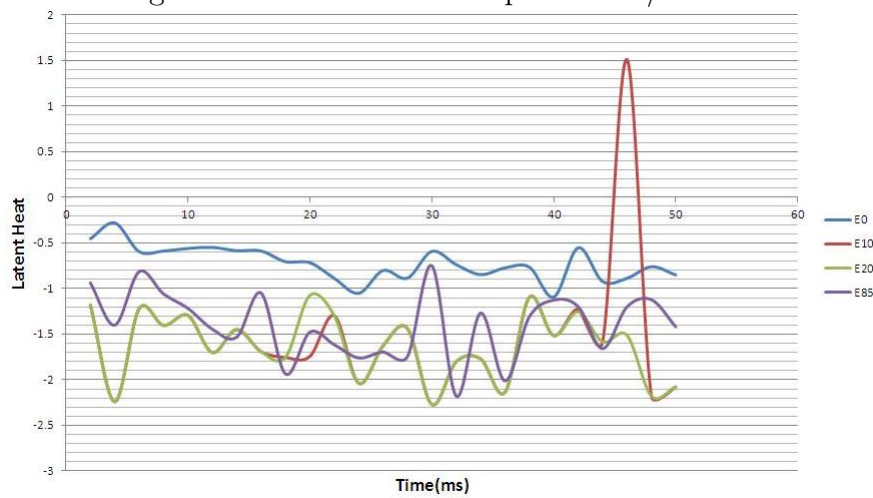
Figure 4.21: Test Case 4: Latent Heat v/s Time

4.4 Multiple Droplet Evaporation: Test Cases

In this section, 4 test cases has been executed for ethanol composition i.e.E0, E10, E20 and E85 with varying Temperature at inlet keeping the droplet temperature(T_D=300 K).Simulations has been performed for the time step of 10^{-8}sec. Here the 15 Droplets has been taken in the rectangular grid flow domain, in which the flow domain is similar to Single Droplet Evaporation Model Cases. Here bottom is the inlet where inlet velocity, V_{in}=30 m/sec is the boundary condition used. Outlet is at the top side where pressure
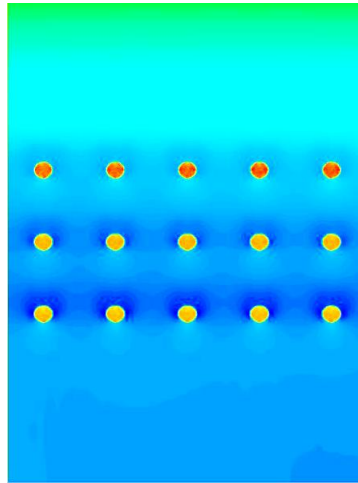
Figure 4.22: Multi Droplet Flow Domain

outlet boundary condition is used and on the side walls, symmetry is taken as boundary condition. This case is generally studied under the inline flow system where all the droplets are in a regular lanes.

Here we are concentrating on the evaporation behavior of droplets. The multiple droplet flow domain is shown in the Fig.[4.22]. All the 15 droplets have same dia D=$20\mu m$ separated from each other in x and y direction with $80\mu m$ distance. The Droplet nearer to the side walls has been kept at distance of $40\mu m$. In case of Multi Droplets, the evolution of droplets is different from the evolution of Single Droplet Cases.
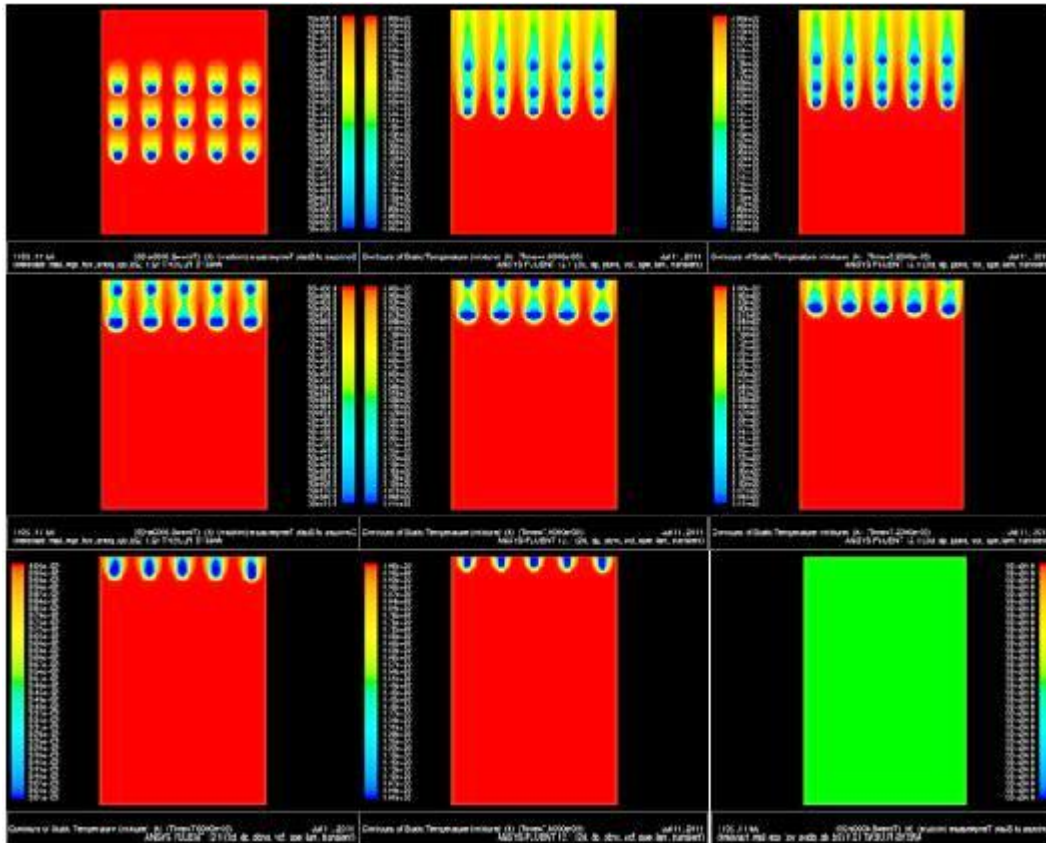

Figure 4.23: Evaporation of Droplets w.r.t time

In the above Fig.[4.23], the simulated graphics for static temperature shows the evaporation behaviour of multidroplets in the flow domain.

4.4.1   Test Case 1

At **Inlet Temperaure=400K**

In this case, inlet temperature is taken as 400K with inline droplets flow domain. Maximum forces are acting on the drop 1 as compared to the droplet 2 and 3 which are far away from the inlet of the flow domain,Hence the decrease in droplet size or volume up-to certain time steps has been shown in the in Fig.[4.24],Fig.[4.25],Fig.[4.26]for Drop1, Drop2,Drop3.
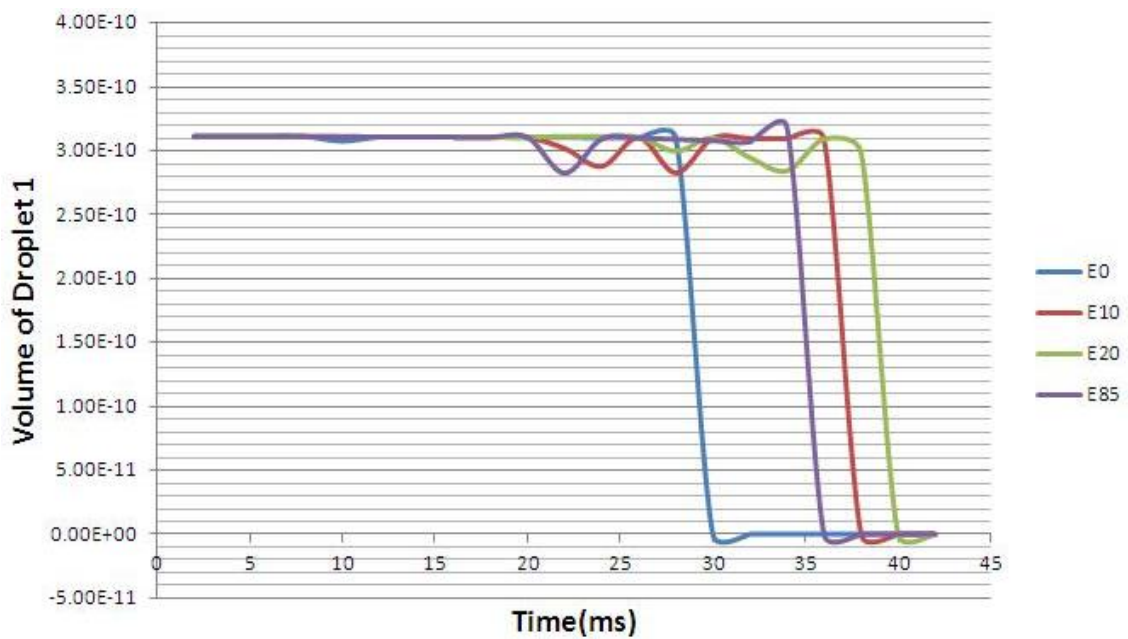

Figure 4.24: Test Case 1: Volume of Drop 1 v/s Time

Fig.[4.24] shows the behavior of drop1 for various compositions has been compared and it shows that E0 droplet get diminished at faster rate with respect to others with in a particular time spam.
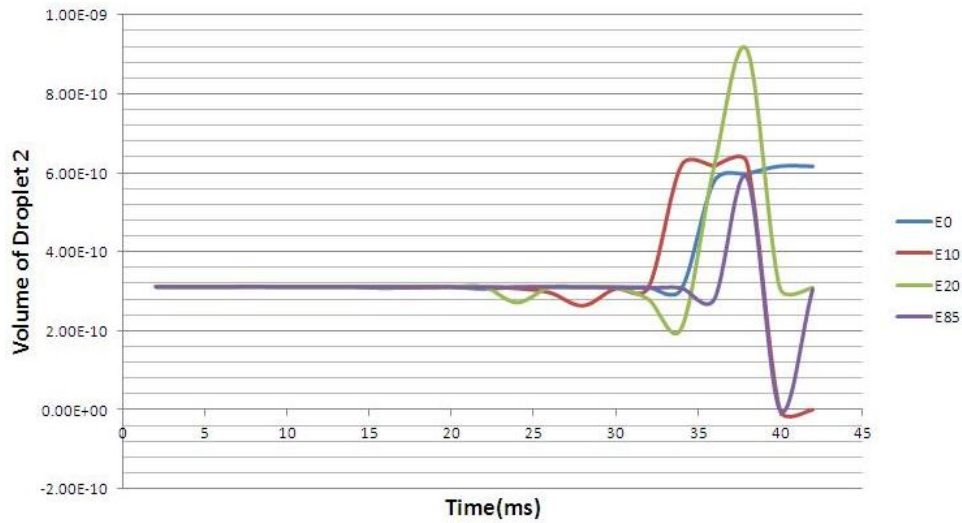
Figure 4.25: Test Case 1: Volume of Drop 2 v/s Time

Fig.[4.25] shows the behavior of drop2 for various compositions. Initially all the compositions have similar volume variations but after some interval of time, the droplet volume get increased because the drop1 (bottom one) get merge into drop2, hence in the plot there is sudden rise in volume instead of decrease in it.
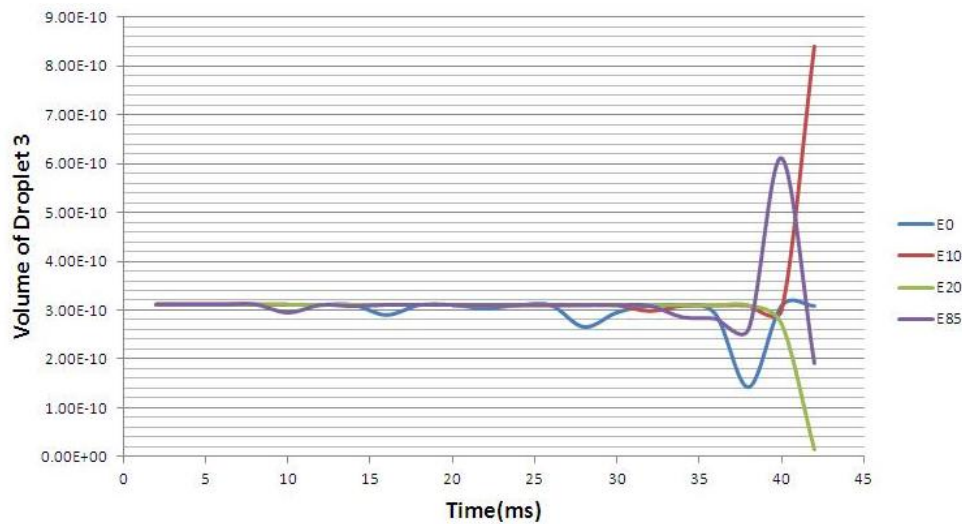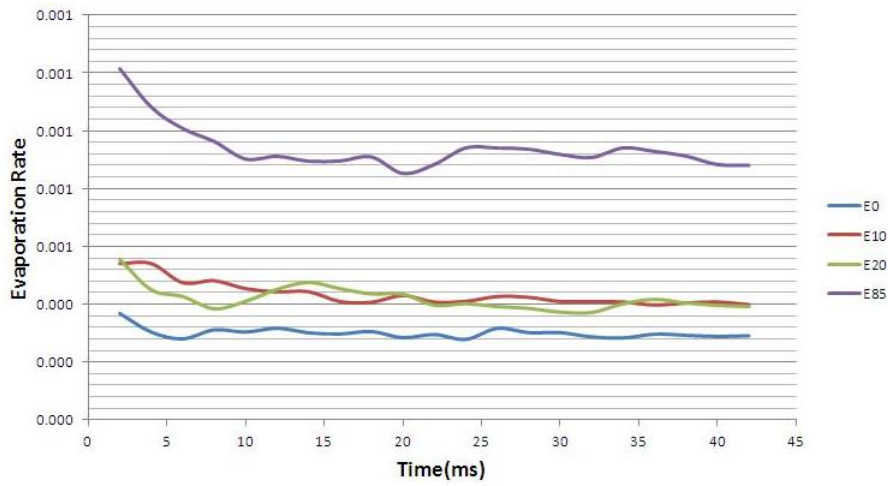

Figure 4.26: Test Case 1: Volume of Drop 3 v/s Time

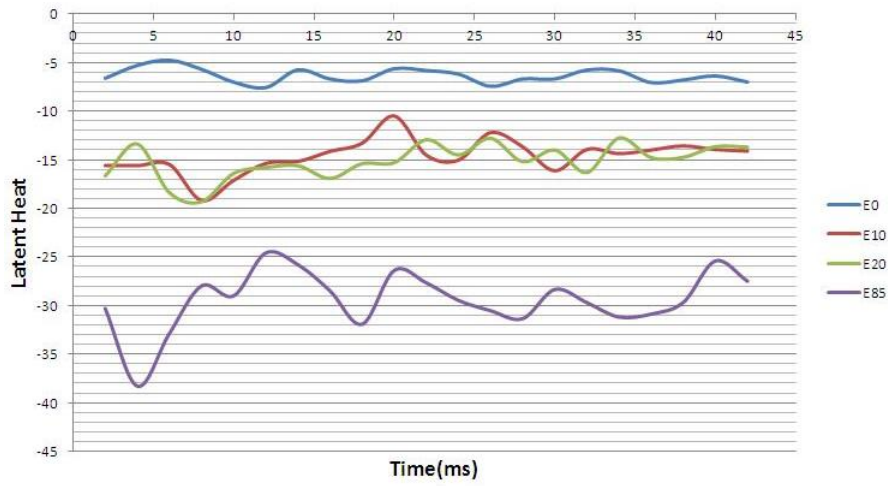Figure 4.27: Test Case 1: Evaporation Rate v/s Time

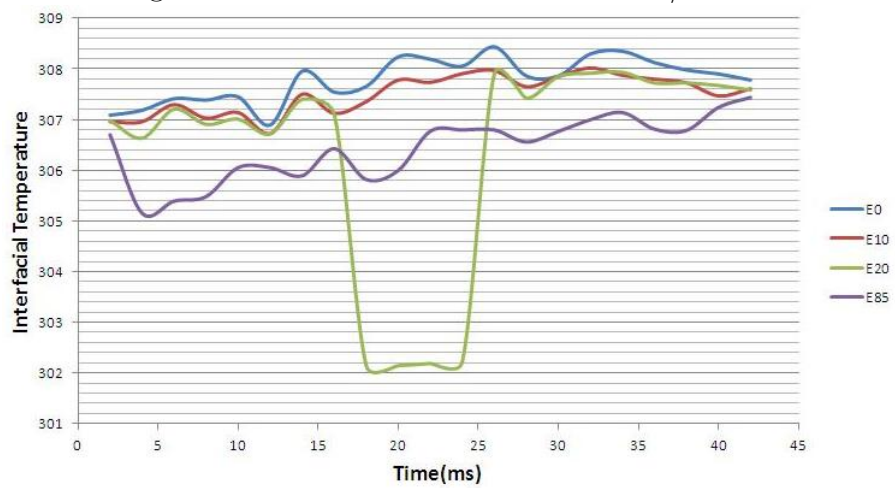Figure 4.28: Test Case 1: Latent Heat v/s Time

Figure 4.29: Test Case 1: Interfacial Temperature v/s Time

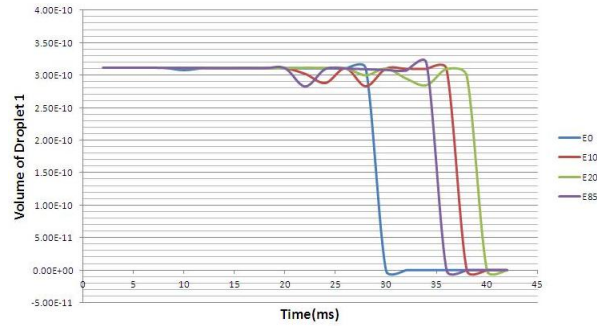### 4.4.2 Test Case 2

At **Inlet Temperaure=500K**

Figure 4.30: Test Case 2: Volume of Drop 1 v/s Time
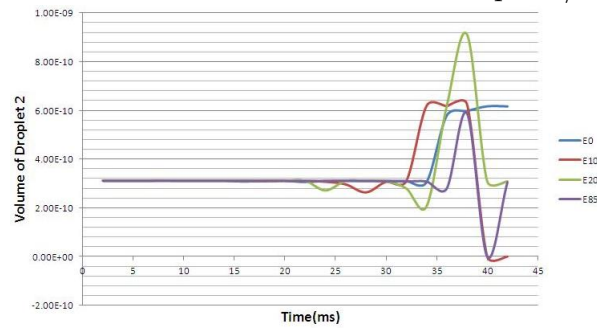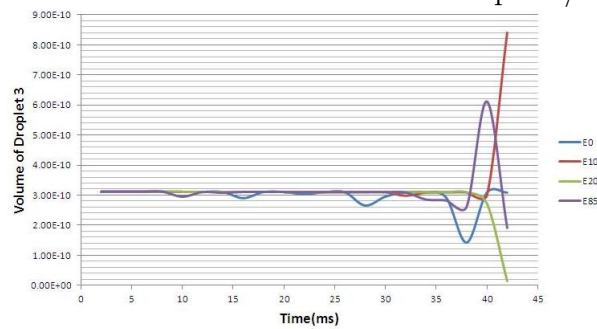

Figure 4.31: Test Case 2: Volume of Drop 2 v/s Time

Figure 4.32: Test Case 2: Volume of Drop 3 v/s Time

Here from the Fig. [4.30], Fig. [4.31], Fig. [4.32] we can see the way drop 1 get diminsh after some in terval and get merge into 2nd drop. This clappsing of drop 1 and 2 is shown by hikes in the plots for drop2 and same in case of drop3.
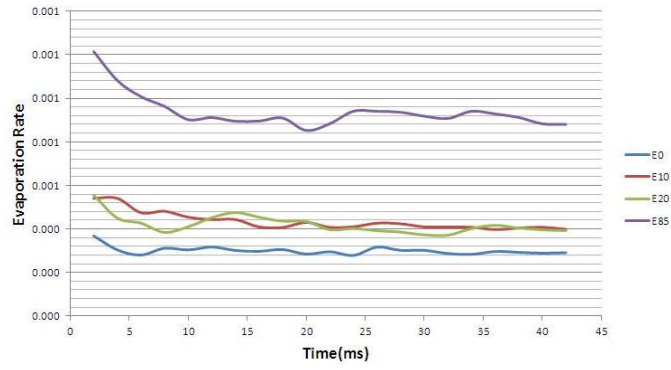
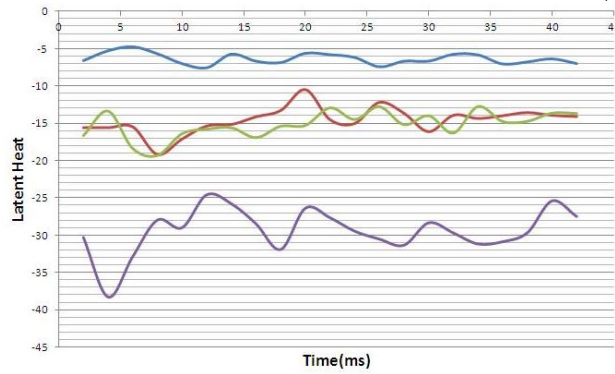Figure 4.33: Test Case 2: Evaporation Rate v/s Time

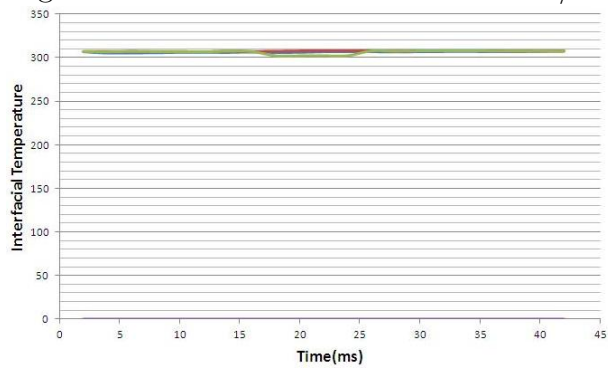Figure 4.34: Test Case 2: Latent Heat v/s Time

Figure 4.35: Test Case 2: Interfacial Temperature v/s Time

Here in the Fig. [4.33], Fig. [4.34] and Fig. [4.35], shows the evaporation rate, latent heat anf Interfacial temperature variation for the E0,E10,E20 and E85 compositions of fuel.

4.4.3   Test Case 3

At **Inlet Temperaure=600K**

Here in Fig. [4.36], Fig. [4.37] and Fig. [4.38], shows the behavior for Latent heat, Interfacial Temperature and Evaporation Rate at inlet temperature of 600 K where all the drops are at temperature of 300K.

Figure 4.36: Test Case 3: Latent Heat v/s Time
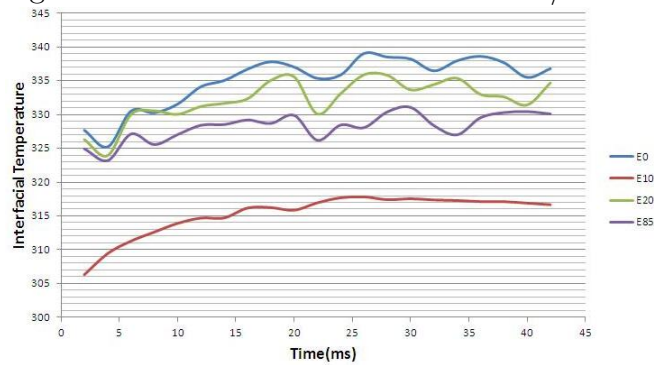
Figure 4.37: Test Case 3: Interfacial Temperature v/s Time
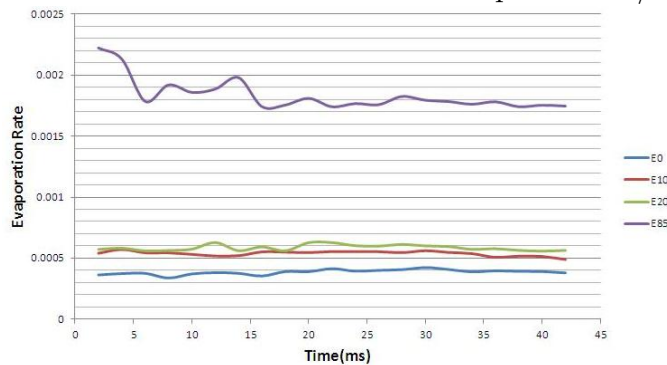
Figure 4.38: Test Case 3: Evaporation Rate v/s Time

4.4.4 Test Case 4

At **Inlet Temperaure=700K**

In this test case the drops are taken at same temperature that is 700K and inlet temperature for the flow domain has been taken as 700.
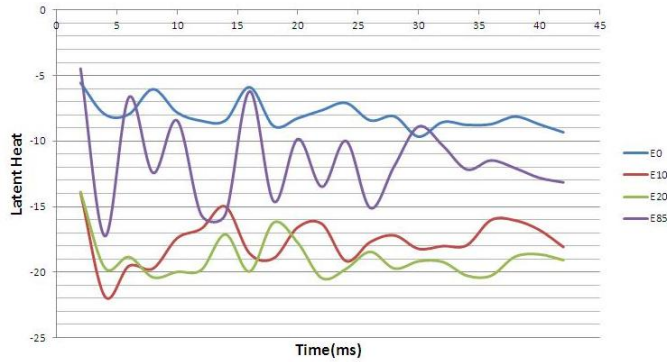

Figure 4.39: Test Case 4: Latent Heat v/s Time

Figure 4.40: Test Case 4: Interfacial Temperature v/s Time
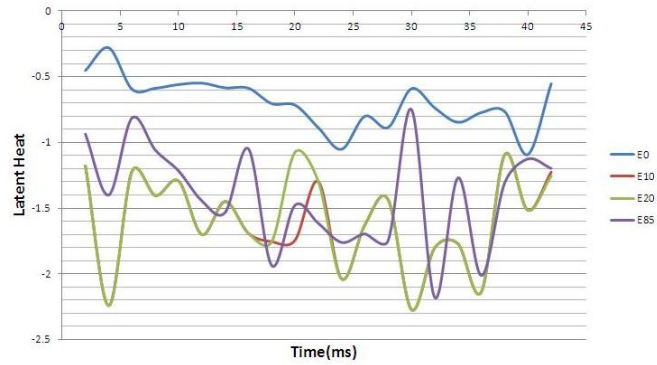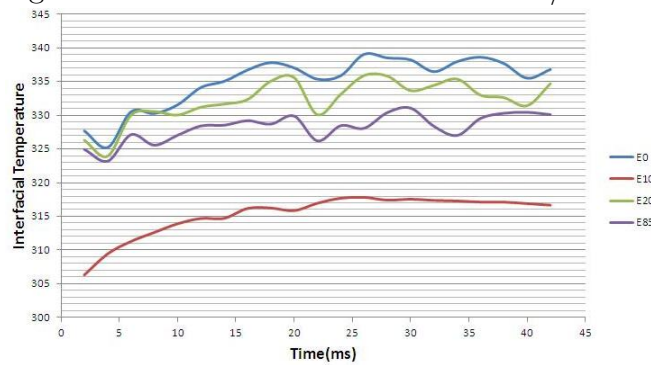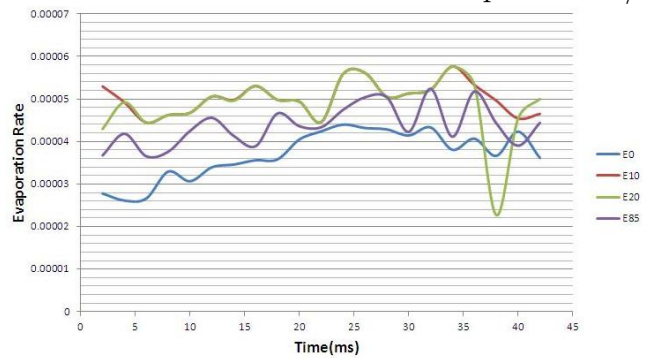

Figure 4.41: Test Case 4: Evaporation Rate v/s Time

Above graphs shows the behavior of E0,E10,E20 and E85 fuels for Evaporation Rate, Interfacial Temperature and Latent Heat.

Chapter 5

Conclusion and Future work

In the study cases, the simulations has been done for Single Droplet Evaporation and Multiple droplet Evaporation Models with in the same flow domain after achieving the Grid Independence study. Calculation for the various parameters like Evaporation Rate, Latent heat, Surface to Volume Ratio, Interfacial Temperature and Volume with respect to time has been done for E0, E10, E20 and E85 compositions of fuel. In case of Single Droplet Evaporation Model, emphasis has been put on Surface to Volume ratio w.r.t to time. However in case of Multi Droplet Evaporation, Instead of Surface to Volume Ratio, study on variation in Volume of individual droplet with respect to time has been done, keeping all the other parameters for the different inlet temperatures as common in both the cases. This is because, In both the cases .i.e. Single and Multiple Droplets , the Evolution of drops are different as in case of Multiple Droplet, the droplet merging has been observed.

In the future work, The validation for E0 fuel droplet i.e. pure composition can be done with conduction taking in account for Single Droplet Evaporation Model. Where as in case of Multiple Droplet Evaporation Model, the flow domain would be extended to some more extent and then cases would be performed further by offsetting the droplets in multiple layers i.e. not inline but segregated drops and then study can be perform on the Evaporation rate Calculation for the droplets i.e. effect of single drop evaporation on other droplets as the droplet layer nearer to the inlet will evaporate much faster as compared to the next one.

Bibliography

[1] Advanced gasoline engine development using optical diagnostics and numerical modeling q M.C. Drake a,*, D.C. Haworth b a Powertrain Systems Research Laboratory, General Motors Research and Development, Warren, MI 48090-9055, USA b Department of Mechanical and Nuclear Engineering, The Pennsylvania State University, University Park, PA 16802-2321, USA Abstract

[2] Heywood J.H., 1988. Internal Combustion Engine Fundamentals, 1st. ed., McGraw-Hill Science.

[3] H. Kronemayer, K. Omerbegovic and C. Schulz, Quantification of the Evaporative Cooling in an Ethanol Spray Created by a Gasoline Direct-Injection System Measured by Multiline NO-LIF Gas-Temperature Imaging, Applied Optics, vol. 46, 2007, pp. 8322-8327

[4] Drake M.C. and Haworth D.C., 2007. Advanced Gasoline Engine Development using optical and numerical modeling. Proc. Combust.. Inst., 31, pp. 99-124

[5] H.P. Trinh, C.P. Chen and M.S. Balasubramanyam, Numerical Simulation of Liquid Jet Atomization Including Turbulence Effects, J. Gas Turbines Power, vol. 129, 2007, pp. 920-928 P. Miles and M. Dilligan, Quantitative In-Cylinder Fluid Composition Measurements Using Broadband Spontaneous Raman Scattering, SAE Technical Paper # 960828, International Congress & Exposition, Feb. 1996, Detroit, MI.

[6] M. Knapp, V. Beushausen, W. Hentschel, P. Manz, G. Grunefeld and P. Andresen, In-Cylinder Mixture Formation Analysis with Spontaneous Raman Scattering Applied

to a Mass-Production SI Engine, SAE Paper Technical Paper # 970827, International Congress & Exposition, Feb. 1997, Detroit, MI .

[7] P.C. Hinze and P.C. Miles, Quantitative Measurements of Residual and Fresh Charge Mixing in a Modern SI Engine Using Spontaneous Raman Scattering, SAE Technical Paper # 1999-01-1106, International Congress & Exposition, March 1999, Detroit, MI.

[8] M. Schtte, H. Finke, G. Grnefeld, S. Krger, P. Andresen, B. Stiebels, B. Block, H. Meyer and W. Hentschel, Spatially Resolved AirFuel Ratio and Residual Gas Measurements by Spontaneous Raman Scattering in a Firing Direct Injection Gasoline Engine, SAE Technical Paper

[9] T. A. Baritaud and T. A. Heinze, Gasoline Distribution Measurements with PLIF in a SI Engine, SAE Technical Paper # 922355, International Fuels & Lubricants Meeting & Exposition, Oct. 1992, San Francisco, CA

[10] B. Deschamps, R. Snyder and T. Baritaud, Effect of Flow and Gasoline Stratification on Combustion in a 4-Valve SI Engine, SAE Technical Paper # 941993, International Fuels & Lubricants Meeting & Exposition, Oct. 1994, Baltimore, MD

[11] J. D. Smith, V. Sick, Quantitative, Dynamic Fuel Distribution Measurements in Combustion-Related Devices Using Laser-Induced Fluorescence Imaging of Biacetyl in Iso-Octane, Proc. Combus. Inst., vol. 31, 2007, pp. 747-755

[12] VH. Neij, B. Johansson and M. Aldn, Development and Demonstration of 2D-LIF for Studies of Mixture Preparation in SI Engines, Combus. Flame, vol. 99, 1994, pp. 449-457 T. Urushihara, T. Nakata, A. Kakuhou and Y. Takagi, Effects of Swirl and Tumble Motion on Fuel Vapor Behavior and Mixture Stratification in Lean Burn Engine, JSAE Review, vol. 17, 1996, pp. 239-244

[13] T. Urushihara, T. Nakata, A. Kakuhou and Y. Takagi, Effects of Swirl and Tumble Motion on Fuel Vapor Behavior and Mixture Stratification in Lean Burn Engine, JSAE Review, vol. 17, 1996, pp. 239-244

[14] H. Hishinuma, T. Urushihara, A. Kakuho and T. Itoh, Development of a Technique for Quantifying In-Cylinder A/F Ratio Distribution Using LIF Image Processing, JSAE Review, vol. 17, 1996, pp. 355-359

[15] C. Schulz and V. Sick, Tracer-LIF Diagnostics: Quantitative Measurement of Fuel Concentration, Temperature and Fuel/Air Ratio in Practical Combustion Systems, Prog. Energy Combus. Sci., vol. 31, 2005, pp. 75-121

[16] L. Zigan, I. Schmitz, A. Flgel, M. Wensing, A. Leipertz, Structure of Evaporating Single- and Multicomponent Fuel Sprays for 2nd Generation Gasoline Direct Injection, Fuel, vol. 90, 2011, pp. 348-363

[17] C. Schulz and V. Sick, Tracer-LIF Diagnostics: Quantitative Measurement of Fuel Concentration, Temperature and Fuel/Air Ratio in Practical Combustion Systems, Prog. Energy Combus. Sci., vol. 31, 2005, pp. 75-121

[18] M. Fujimoto and M. Tabata, Effect of Swirl Rate on Mixture Formation in a Spark Ignition Engine Based on Laser 2-D Visualization Techniques, SAE TEchnical Paper # 931905, International Pacific Conference On Automotive Engineering, Nov. 1993, Phoenix, AZ

[19] M. Fujimoto, K. Nishida, H. Hiroyasu and M. Tabata, Influence of Mixture Stratification Patter non Combustion Characteristics in a Constant-Volume Combustion Chamber, SAE Technical Paper # 952412

[20] M. Knapp, A. Luczak, V. Beushausen, W. Hentschel and P. Andresen, Vapor/Liquid Visualization with Laser-Induced Exciplex Fluorescence in an SI-Engine for Different Fuel Injection Timings, SAE Technical Paper # 961122, International Fuels & Lubricants Meeting & Exposition, May 1996, Dearborn, MI

[21] P. L. Kelly-Zion, J. P. Styron, Chia-Fon Lee, R. P. Lucht, J. E. Peters and R. A. White, Multicomponent Liquid and Vapor Fuel Measurements in the Cylinder of a Port-Injected, Spark Ignition Engine, Symp. (Int.) Combus., vol. 27, 1998, pp. 2111-2117

[22] D.S. Choi, G.M. Choi and D.J. Kim, Spray Structures and Vaporizing Characteristics of a GDI Fuel Spray, J. Mech. Sci. Tech., vol. 16, 2002, pp. 999-100

[23] P. Wieske, S. Wissel, G. Grnefeld and S. Pischinger, Improvement of ....LIEF by Wavelength-Resolved Acquisition of Multiple Images Using a Single CCD Detector Simultaneous 2D Measurement of Air/Fuel Ratio, Temperature Distribution of the Liquid Phase and Qualitative Distribution of The Liquid Phase with the Multi-2D Technique, App. Phy. B: Lasers Optics, vol. 83, 2006, pp. 323-329

[24] E.K. Anderson, A.P. Carlucci, A.D. Risi, D.C. Kyritsis, Synopsis of Experimentally Determined Effects of Electrostatic Charge on Gasoline Sprays, Energy Conversion Management, vol. 48, 2007, pp. 2762-2768

[25] P.G. Aleiferis, J. Serras-Pereira, Z. van Romunde, J. Caine and M. Wirth, Mechanisms of spray formation and combustion from a multi-hole injector with E85 and gasoline, Combust. Flame, vol. 157 2010 pp. 735756

[26] 26 K.H. Lee, C.H.Lee and C.S. Lee, An experimental Study on the Spray Behaviour and Fuel Distribution of GDI Injectors Using the Entropy Analysis and PIV Method, Fuel, vol. 83, 2004, pp. 971-980

[27] S. Moon, E. Abo-Serie and C. Bae, The Spray Characteristics of a Pressure-Swirl Injector with Various Exit Plane Tilts, Int. J. Multiphase Flow, vol. 34, 2008, pp. 615-627

[28] Drop and spray formation from a liquid jet.S.P.Lin/Mechanical and Aeronautical Engg. Deptt., Clarkson University,Potsdam. New York 19699:email:gw02@sun.soe.clarkson.edu. R.D.Reitz, Mechanical Engineering Deptt.,University of Wisconsin, Madison,Wisconsin,53706;email:reitz@engr.wisc.edu.

[29] LES Simulation of internal Flow and Near-feild Spray Structure of an Outward opening GDi Injector and Comparison with Imaging Data,D.Robart and W.Reckers. Delphi Customer Technology Centre, G.-D.Luxembourg. H.Weller Open-CFD,UK.

[30] Evaporation Characteristic of multi component Liqiud.Katsuhiro Okamoto a,Norimichi Watanabe a, Yasuaki Hagimoto a, Koji Miwa a, Koji Miwa a, Hideo Ohanti b Yokohama National University, 79-7, Tokiwadai, Hodogaya-ku,Yokohama City, K anagawa 240-8501, Japan.

[31] N. Assanis, S. J. Hong, A. Nishimura, G. Papageorgakis and B. Vanzieleghem, Studies of Spray Breakup and Mixture Stratification in a Gasoline Direct Injection Engine Using Kiva-3V, J. Eng. Gas Turbines Power, vol. 122, 2000, pp 485-492

[32] M.S. Balasubramanyam and C.P. Chen, Modelling Liquid Jet Breakup in High Speed Cross-Flow with Finite-Conductivity Evaporation, Int. J. Heat Mass Transfer, vol. 51, 2008, pp. 38963905

[33] L. Zhang and S.C. Kong, Modelling of Multi-Component Fuel Vaporization and Combustion for Gasoline and Diesel Spray, Chem. Eng. Sci., vol. 64, 2009, pp. 3688-3696

[34] R.V.R. Pandya and F. Mashayek, Two-Fluid Large-Eddy Simulation Approach for Particle-Laden Turbulent Flows, Int. J. Heat Mass Transfer, vol. 45, 2002, pp. 47534759

[35] S.V. Apte, M. Gorokhovski, P. Moin, LES of Atomizing Spray with Stochastic Modeling of Secondary Breakup, Int. J. Multiphase Flow vol. 29, 2003, pp. 15031522

[36] T.G. Almeida and F.A. Jaberi, Large-Eddy Simulation of a Dispersed Particle-Laden Turbulent Round Jet, Int. J. Heat Mass Transfer, vol. 51, 2008, pp. 683695

[37] J.M. Senoner, M. Sanjos, T. Lederlin, F. Jaegle, M. Garca, E. Riber, B. Cuenot, L. Gicquel, H. Pitsch and T. Poinsot, Eulerian and Lagrangian Large-Eddy Simulations of an Evaporating Two-Phase Flow, C. R. Mecanique, vol. 337, 2009, pp. 458468

[38] W.P. Jones, S. Lyra and A.J. Marqui, Large Eddy Simulation of a Droplet Laden Turbulent Mixing Layer, Int. J. Heat Fluid Flow, vol. 31, 2010, pp. 93100

[39] F.A. Jaberia and F. Mashayek, Temperature decay in two-phase turbulent flows, Int. J. Heat Mass Transfer, vol. 43, 2000, pp. 993-1005

[40] T.G. Almeida and F.A. Jaberi, Direct Numerical Simulations of a Planar Jet Laden With Evaporating Droplets, Int. J. Heat Mass Transfer, vol. 49, 2006, pp. 21132123

[41] R. Lebas, T. Menard, P.A. Beau, A. Berlemont and F.X. Demoulin, Numerical simulation of primary break-up and atomization: DNS and modelling study, Int. J. Multiphase Flow, vol. 35, 2009, pp. 247260

[42] M. Ishii and T. Hibiki, Thermo-Fluid Dynamics of Two-Phase Flow, 2nd ed., Springer, 2010

[43] D. Lakehal, M. Meier and M. Fulgosi, Interface Tracking Towards the Direct Simulation of Heat and Mass Transfer In Multiphase Fows, Int. J. Heat Fluid Flow, vol. 23, 2002, pp. 242257

[44] Trinh, H.P., Chen, C.P. and Balasubramanyam, M.S., 2007. Numerical Simulation of Liquid Jet Atomization Including Turbulence Effects. J. Eng. Gas Turbines Power, 129, pp. 920-928.

[45] Schmel, R., Rosskamp, H., Willmann, M. and Wittig, S., 1999. CFD Analysis of Spray Propagation and Evaporation Including Wall Film Formation and Spray/film Interactions. Int. J. Heat Fluid Flow, 20, pp. 520-529.

[46] Rizk, N.K., Chin J.S. and Razdan, M.K., 1997. Modeling of Gas Turbine Nozzle Spray. J. Eng. Gas Turbines Power, 119, pp. 34-44.

[47] A.K. Agarwal, Biofuels (Alcohols and Bio-diesel) Applications as Fuels for Internal Combustion Engines, Prog. Energy Comb. Sci., vol. 33, 2007, pp. 233-271.

[48] R.K. Niven, Ethanol in Gasoline: Environmental Impacts and Sustainability Review Article, Renewable Sustainability Energy Rev., vol. 9, 2005, pp. 535-555

[49] T. Wallner, S. A. Miers, S. McConnell, A Comparison of Ethanol and Butanol as Oxygenates Using a Direct-Injection, Spark-Ignition Engine, J. Eng. Gas Turbines Power, 2009, vol. 131, 032802

[50] Ranz and Marshall, 1952; Faeth, 1977; Law,1982; Givler and Abraham, 1996)

[51] Kadota and Hiroyasu, 1976; Sato, 1993; Nomura et al., 1996).

[52] Law, 1978; Randolph et al., 1986; Arias-Zugasti and Rosner, 2003; Morin et al., 2004

[53] oungs, D.L., "Time-Dependent Multi-Material Flow with Large Fluid Distortion," Numerical Methods for Fluid Dynamics, Academic Press, 1982.

[54] Patankar, S.V., Numerical Heat Transfer and Fluid Flow, Hemisphere Publishing Corp., Washington, 1980. Versteeg, H.K. and Malalasekra, W., An Introduction to Computaitonal Fluid Dynamics: The Finite Volume Method, Addison Wesley Longman, Inc., London, 1995.

[55] Youngs, D.L., "Time-Dependent Multi-Material Flow with Large Fluid Distortion," Numerical Methods for Fluid Dynamics, Academic Press, 1982.

[56] Hirt, C.W. and Nichols, B.D., "Volume of Fluid (VOF) Method for the Dynamics of Free Boundaries," Journal of Computational Physics, 39, 1981, pp. 201-225

[57] Crank, J., Free and Moving Boundary Problems, Clarendon Press, Oxford, 1984.

[58] Pericleous, K.S., Chan, K.S., and Cross, M., "Free Surface Flow and Heat Transfer in Cavities: The SEA Algorithm," Numerical Heat Transfer, Part B, 27, 1995, pp. 487-507.

[59] Ashgriz, N. and Poo, J.Y., "FLAIR: Flux Line-Segment Model for Advection and Interface Reconstruction," Journal of Computational Physics, 93, 1991 pp. 449-468.